

Optimization of Conditions for Endothelial Seeding of Microfluidic Devices with Long
Branching Networks and Small Channel Dimensions

by

Kevin Zhao

Department of Biomedical Engineering
Duke University

Date:

Approved:

George Truskey, Supervisor

David Katz

Lori Setton

Thesis submitted in partial fulfillment of
the requirements for the degree of Master of Science in the Department of
Biomedical Engineering in the Graduate School
of Duke University
2013

ABSTRACT

Optimization of Conditions for Endothelial Seeding of Microfluidic Devices with Long
Branching Networks and Small Channel Dimensions

by

Kevin Zhao

Department of Biomedical Engineering
Duke University

Date: _____

Approved:

George Truskey, Supervisor

David Katz

Lori Setton

An abstract of a thesis submitted in partial
fulfillment of the requirements for the degree
of Master of Science in the Department of
Biomedical Engineering in the Graduate School of
Duke University

2013

Copyright by
Kevin Tengkun Zhao

Abstract

Many hematologic diseases may have interactions with proteins and endothelium within small microvascular environments that are currently hard to understand. These effects are hard to produce *in vitro*, and relevant studies performed *in vivo* are difficult to image and evaluate at high resolutions. In order to better understand these phenomena, *in vitro* models with optically clear material should be developed that act as platforms for higher power imaging and analysis.

Microfluidic devices made out of polydimethylsiloxane (PDMS) bonded to glass provide this platform and are capable of generating channels of long length (>2.5 cm from inlet to outlet) and of microvascular size (<30 microns). However, current methods of seeding endothelial cells into devices of such dimensions have proven to be very difficult to perform.

One goal of this thesis is to develop a new and reproducible method of seeding endothelial cells into microfluidic devices of many branching networks and small channel dimensions. To examine conditions that lead to optimal seeding, we fabricated a microfluidic device that contains five sets of binary diverging junctions; starting from an inlet of 1000x30 micron dimensions, the flow path splits into a total of 32 small channels of 20x30 micron dimensions. The total distance from inlet to outlet is 3 cm and each channel length is 0.4 cm. We found that traditional flow-in seeding methods are not very effective for long channel networks in which the smallest size is 20x30 microns or less, with poor cell attachment and clogging at junctions being among the biggest hindrances to successful seeding.

Taking all of these factors into account, we developed a reproducible seeding method by dynamically adjusting flow-rates during infusion and using high cell concentrations. This enabled successfully seeding and the formation of confluent layers of endothelial cells lining the inner surfaces of the channels. By utilizing high cell concentrations (3.5-7.5 million cells/mL) of young

endothelial cells, we were able to reduce flow rates to allow for attachment and increase flow rates to shear away clogs at junctions and within the smallest channels. After sufficient initial coverage was generated throughout the device, the device was incubated for thirty minutes to allow for secure cell attachment and any excess aggregates within the device were then sheared away at high flow rates. This process was repeated again after a couple days to clear out any remaining aggregates. Development of the device for 3-4 days in an incubator with constant media flow after seeding helped the endothelial cells to grow into a confluent monolayer within the channel walls of the device.

A second goal is to perform initial studies of flow of sickle cells within endothelialized channels. To test the function of the endothelium in the microfluidic device, samples of recessive HBSS sickle cell blood were allowed to flow into the channels. The flow paths taken by the cells were heavily influenced by the shape, size, and height of endothelial protrusions from the channel walls. In some of the wider channels, the effects of endothelial protrusions were so great that multiple small, enclosed flow paths formed within individual channels, resulting in the creation of flow networks within these individual channels. Finally, after extended flow periods, aggregations formed in a scattered fashion across the endothelium of larger channels that served as high-resistance buildups for further flow into the device.

Contents

Abstract.....	iv
List of Tables	viii
List of Figures.....	ix
Acknowledgements.....	xi
1. Chapter I: Introduction.....	1
1.1 Goals.....	1
1.2 Seeding and Producing Confluent Layers of Endothelial Cells in Microchannels	2
1.3 Sickle Blood Hemodynamics	6
2. Chapter II: Methods	8
2.1 Device Creation.....	8
2.2 Device Seeding.....	13
2.2.1 Myers et al. Protocol	14
2.2.2 Variable Flow Protocol.....	17
2.3 Calculations of Flow Rate, Shear Stress, and Reynolds Number within Channels.....	26
2.4 Imaging Seeded Devices	30
2.5 Sickle Blood Flow into Seeded Devices	31
3. Chapter III: Results	33
3.1 Results Obtained Using the Myers et al. Protocol.....	33
3.2 Need for “Variable Flow”	36
3.3 Seeding Results	39
3.4 Cell Attachment and Growth Mechanics	42
3.5 Cell Concentration Values and Cell Properties	44
3.6 Effects of Dextran and Trypsin, Incubation Lifetime of Confluent Devices	49
3.7 Summary of Test Conditions.....	53

3.8 Brightfield Imaging	54
3.9 Immunofluorescent Imaging	55
3.10 Cell Coverage at Confluence.....	54
3.11 Sickle Blood Flow Results	55
4. Chapter IV: Conclusion	64
4.1 Future studies	65
Appendix A: Device Creation Protocol	67
Appendix B: Blood Flow Experiment Protocol.....	78
References.....	83

List of Tables

Table 1: Flow Rates for Cell Attachment and Declogging	23
Table 2: Shear Stress on Channel Walls with No Dextran in Media	28
Table 3: Shear Stress on Channel Walls with Dextran in Media	28
Table 4: Reynolds Number within Channels without Dextran	29
Table 5: Conditions used for infusion and their respective seeding results	53

List of Figures

Figure 1: Seeded device from Zhang et al.	3
Figure 2: Seeded device from Tsai et al.	3
Figure 3: Seeded device from Esch et al.	4
Figure 4: Seeded device from Rosano et al.	4
Figure 5: Channel pattern.	8
Figure 6: Punching holes through a device.	11
Figure 7: Bonded microfluidic devices and device sizes	12
Figure 8: Incompletely bonded device.	13
Figure 9: Tubing and needle setup.	17
Figure 10: Elimination of air bubbles when connecting tubing to a device.	19
Figure 11: Magnetic stir bar inside syringe	21
Figure 12: Image of variable flow setup	22
Figure 13: Image of sickle flow setup.	32
Figure 14: Clogging within 50 to 20 micron channel junctions.	34
Figure 15: Clogging within 50 to 20 micron channel junctions at small flow rate.	34
Figure 16: Insufficient cell growth within a device	35
Figure 17: Initial seeding results for 5,000,000 cells/mL	39
Figure 18: Early confluency within microchannels	39
Figure 19: Percent coverage of smallest channels vs. infusion concentration	41
Figure 20: Cell attachment within larger and smallest channels during seeding	43
Figure 21: Minimum seeding concentration	45
Figure 22: Threshold seeding concentration for leakage within the smallest channels	46
Figure 23: Seeding images of old cells vs. young cells	48

Figure 24: Effects of 0.1% and 0.15% Trypsin on Cell Detachment for Seeding	51
Figure 25: Exceeded Maximum Incubation Lifetime	52
Figure 26: Brightfield Images of Confluency	54
Figure 27: Confocal Images of Confluency (50 to 20 and 100 to 50 micron junctions)	55
Figure 28: Confocal Images of Confluency (20 micron channel and 50 to 20 micron junction) ..	55
Figure 29: Confocal Fluorescent Images of Confluency (200 to 100 micron junction)	56
Figure 30: Confocal Fluorescent Images of Confluency (400 to 200 micron junction)	56
Figure 31: Cell Densities within Channels	57
Figure 32: Sickle Flow in Larger Channels	58
Figure 33: Sickle Aggregations in Larger Channels (Post-Flow).....	59
Figure 34: Sickle Flow in Small Channels	60
Figure 35: Sickle Aggregations in Small Channels (Post-Flow)	61
Figure 36: Leakage at Device Inlet	62

Acknowledgements

I would like to give special thanks to Tracy Cheung for training and helping me with cell culture and passaging, fixing and staining cells, and fluorescent imaging. She provided incredibly valuable input for me and helped me with virtually every step of the cell culturing and staining processes. Without her, none of this would be possible.

I would also like to give special thanks to Matt Rinehart for helping me image my cells and giving me valuable input for both cell seeding and subsequent device development. He went through extensive efforts to help me get better quality images of my work, some of which are shown in this thesis.

Finally, I would like to thank Professor David Katz, Professor Lori Setton, and Professor George Truskey for the advising roles they played in helping me to produce this thesis. I have taken classes with all of them and the material I learned in these classes has made my stay here at Duke well worth it. I have learned how to think outside the box from Professor Katz and Setton, and Professor Truskey has personally advised me the entire way for my time on this project.

Chapter I: INTRODUCTION

Hematologic diseases have a variety of effects on blood, such as causing anemia and red cell damage, altering the oxygen-absorbing capabilities of red blood cells, and even affecting the shape of the red blood cells themselves ¹⁻³. What happens when blood associated with these diseases flows within small microvascular environments is known on a qualitative scale, but the actual mechanics of cellular interaction inside these microenvironments during blood flow are largely unknown ^{4, 5}. For example, vaso-occlusion occurs for sickle cell disease within small capillaries, but there is a limited understanding of the actual biomechanics of aggregate formation and the interactions of sickle cells with environmental factors under physiological flow conditions. *In vivo* methods of study are currently very hard to image at high power and are thus unable to contribute the data necessary to come to conclusions regarding flow biomechanics within these microenvironments ⁵. Thus, *in vitro* models that can be effectively imaged can be used to examine hematologic phenomena in small channels. Microfluidic devices made with polydimethylsiloxane (PDMS) offer an optically clear platform through which these models can be developed ⁶. Currently there are very few, if any, reproducible methods to effectively seed these microfluidic devices with endothelial cells in order to generate physiologically-relevant microvascular environments.

1.1-Goals

The first goal of this thesis is to develop a reproducible method of seeding endothelial cells into microvascular-sized microchannels. This allows for the creation of *in vitro* vessel environments that closely mimic *in vivo* conditions. The second goal of this thesis is to perform a hematological study of sickle cell perfusion through these endothelialized channels. Since the flow mechanics and adhesion of sickle cell blood within small microvascular environments are poorly understood,

sickle blood will be used as the test medium to flow within these channels. Flow videos obtained from this study will generate insight into the biomechanics of sickle blood, such as indicators of binding affinity of sickle cells to endothelium and detachment forces of sickle cell aggregates within small channels.

1.2-Seeding and Producing Confluent Layers of Endothelial Cells in Microchannels

The field of microfluidics has been developing over the recent years, with advancements being made in various areas such as micromixing via electric currents ⁷, branching with hundreds of channels and valves ⁸, and even the synthesis of nanostructures within channels ⁹. However, using microfluidics as a platform to simulate flow in endothelialized microvessels that mimic arterioles, venules, and capillaries is relatively nascent. If branching microfluidic channels that are sufficiently small (<30 microns on all sides) can be seeded with endothelial cells in a reproducible manner, this would provide an inexpensive yet cutting-edge way to engineer small microvascular networks that mimic the *in vivo* conditions of endothelium. Devices with these features can provide great insight as to what happens within small microvascular networks under varying flow conditions and for different hematologic diseases, which previously could not be done.

There have been a few of publications that depict endothelial seeding inside branching microchannels. A study at the University of Toronto in 2013 performed seeding into a device that eventually branched into four 100x100 micron channels ¹⁰. A couple of studies at Emory University in 2012 show endothelialization within channels as small as 30x30 microns ^{11, 12}. Furthermore, a study at Cornell University in 2011 shows endothelial seeding of square and semi-circular 60x45 micron single channels ¹³. Another striking study was performed at Temple

University where physiologically- shaped channels of 50-100 micron depths and similar widths were seeded with endothelial cells ¹⁴. Images from these studies are shown below (Figs. 1-4).

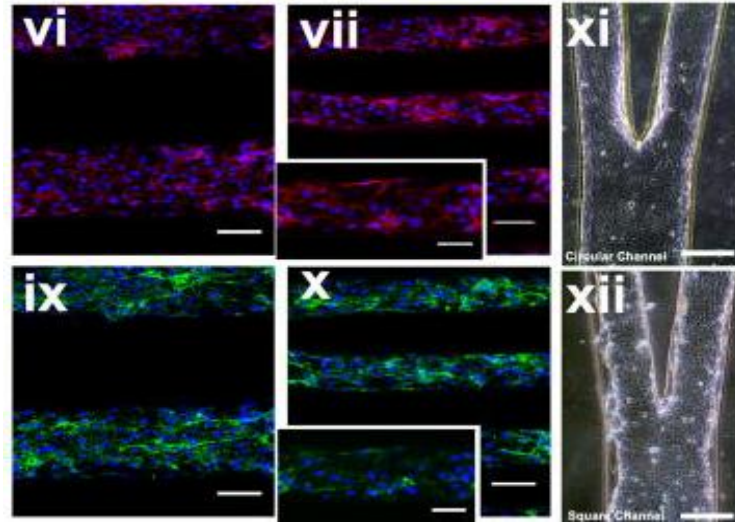


Figure 1: Images of 100x100 micron channels from Zhang et al (2013) ¹⁰. In images VI and VII, VE-cadherin is stained red to show contact between endothelial cells and DAPI is stained blue to show cell nuclei. In images IX and X, Von-Willebrand factor is stained green in addition to DAPI blue staining. In pictures XI and XII, brightfield images are shown of junctions leading into 100 micron channels.

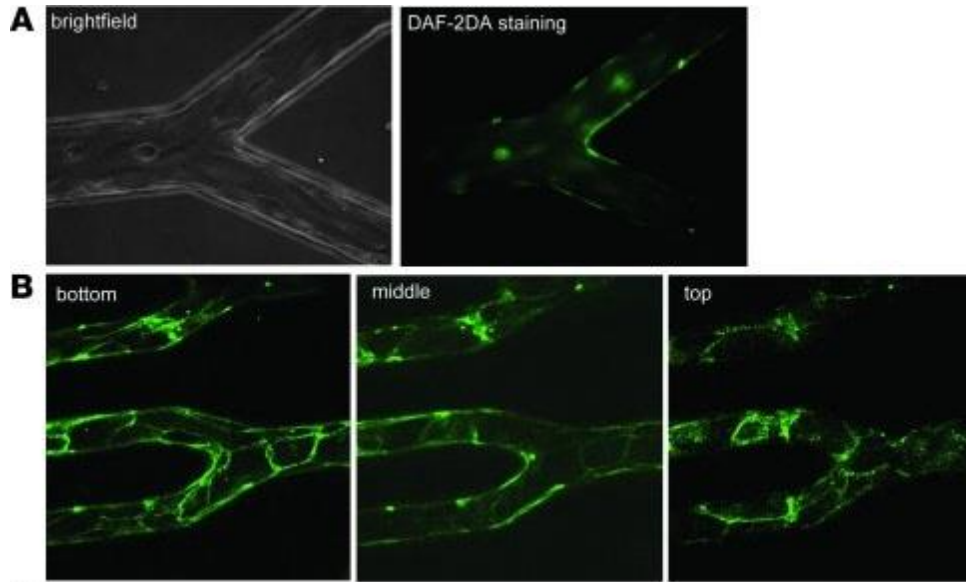


Figure 2: Images of 30x30 micron junctions from Myers et al. and Tsai et al. (2012) ^{11, 12}. (A) Brightfield images showing that endothelial cells are spread throughout the junction and extending into the channel. (B) Fluorescently stained junctions for VE-cadherin showing cells are in contact with one another.

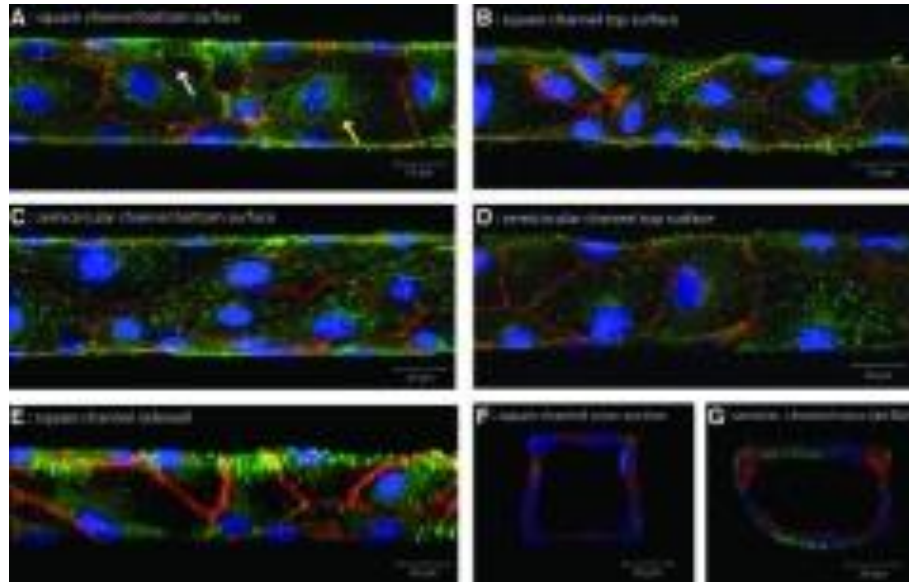


Figure 3: Images of both square and semicircular channels from Esch et al. (2011) ¹³ showing vinculin (green) and VE-cadherin localization (red) in images A-E. Images F and G show cross-sectional views of both types of channels.

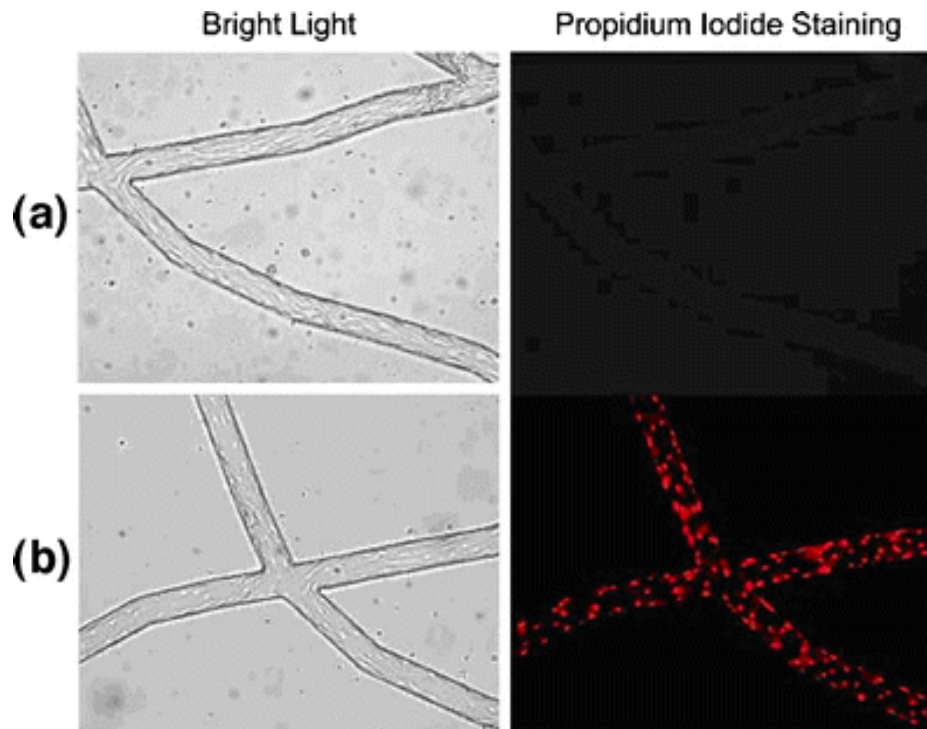


Figure 4: Images of physiologically shaped channels from Rosano et al. (2009) ¹⁴ showing confluent cell seeding. The left panel depicts endothelial cells in brightfield while the right panel shows Propidium Iodine staining to fluorescently visualize cell nuclei.

All of these studies generated confluent endothelial monolayers that covered the entire inner surfaces of their respective device channels in channels. The Myers et al. and Tsai et al. studies generated monolayers in channels as small as 30x30 microns^{11, 12}. VE-cadherin staining indicates that the endothelial cells are in contact with each other. They utilized constant flow rates in order to infuse an unmixed cell solution into microfluidic devices over a period of a few hours. Afterwards, these devices were incubated and media flowed through the devices over the course of a few days in order to allow cells to grow and form confluent layers. However, while the Zhang¹⁰, Esch¹³, and Rosano¹⁴ studies channels with dimensions larger than endothelial cells in suspension (the dimensions of 100x100 microns and 60x45 microns are sufficiently large, especially without branching networks), the Myers et al. and Tsai et al.^{11, 12} studies have channels of microvascular dimensions and a binary branching network. These are more difficult to seed and are very similar in shape to the channels of devices we used in this study. In addition, one of our major goals was not only to seed small channel widths, but to also generate confluent monolayers in very long channel networks that are multiple centimeters in length. As is discussed in the Results section of this thesis, we were unable to utilize the Myers et al. and Tsai et al.^{11, 12} protocol for our goal of seeding long networks of microvascular dimensions. This could in part be due to the fact that their protocol is perhaps more optimized for short networks (on the order of millimeters). During our seeding trials using their protocol for longer channel patterns, there were at most a few clusters of cells lined within the larger channels, and small clusters clogging the forks gating the entry to the smallest channels. One possible reason for this difference is that ECs in this study tended to form clusters of cells during seeding, and the distance that needs to be covered while traveling through long channels contributes to their attachment and clogging behaviors. The seeding of clusters is explored in more detail in the Results.

Thus, the first goal of this thesis is to create a reproducible protocol for seeding endothelial cells into long channels (3 cm or greater in length from inlet to outlet) that are of microvascular size (<30 micrometers on all sides) and form confluent monolayers within three days. During this process, factors such cell concentration, flow rates, and growth time within channels will be examined and optimized for cell seeding.

1.3- Sickle Blood Hemodynamics

Sickle cell disease results from the presence of aberrant hemoglobin S (Hb S) with respect to one single amino acid substitution in the hemoglobin gene, in which glutamic acid at the sixth position is replaced by valine ¹⁵. This mutation causes hemoglobin to lose deformability under low oxygen conditions in the venules and red cells to turn into rigid sickle-like shapes. The anemia itself is exacerbated by increased clearance levels of sickled red cells within the body, which decreases the overall hemoglobin count within blood and the overall oxygen content. This anemia, in turn, causes deoxygenation within the blood and leads to more sickle cells to form. Intercellular aggregation is caused by the geometric stiffness of the cells, which cause clogging and vaso-occlusion within small vessels. Moreover, immature reticulocytes within the blood, generated at higher quantities due to anemic conditions, adhere to endothelial cells and white blood cells ¹⁶, which compounds the effects of their ease of intercellular aggregation.

Sickle cell adhesion to endothelium depends on a variety of factors, such as erythrocyte density and shape, adhesion molecules associated with platelets and other red cells, activation of the endothelium, and even hydration levels ¹⁷. Deactivation of P-selectin, a leukocyte adhesion molecule, causes decreased levels of sickle-cell aggregation within a mouse model of sickle cell disease¹⁸. Another study shows that the erythrocyte phosphatidylserine, an endothelial adhesion phospholipid, plays a critical role in the adhesion of sickle cells to unactivated endothelium ¹⁹. In

conjunction, phosphatidylserine mediates sickle cell adhesion to lung endothelium ²⁰.

Furthermore, although red blood cells and sickle cells do not differ too greatly in adhesion likelihood to the endothelium under static conditions, the required tangential detachment force for sickled cells is over one hundred times greater than for regular endothelial cells, which contributes to sickle cell aggregations along the endothelial wall ²¹.

As mentioned in the introduction, there have been few *in vitro* studies under conditions that match microvascular physiological environments, operated under physiological flow properties, and conducted within capillary, arteriole, and venule-like geometries (in fact, the protocol found in Tsai et al. and Myers et al. (studies from the same institution) ^{11, 12} is the only one). Thus, the other focus of this thesis is to perform an initial study on the vaso-occlusive properties of sickle cell blood within a microfluidic device that is confluent with endothelial cells. We will note the patterns of bolus formation, the flow paths of sickle cells within the device, and the aggregation effects of sickle blood in channels of various dimensions. More importantly, our aim is to show that this platform can be used in a variety of future tests in order to better understand the mechanics of hematologic diseases within microvascular environments.

Chapter II: METHODS

2.1- Device Creation

For a fully-detailed protocol, completely with pictures, please see Appendix A

Network Pattern- Imprinted onto Silicon Wafer

The microfluidic device used in this thesis contains a branching network that starts with a channel width of 1000 microns and, through 5 sets of binary diversions, branches into 32 small channels with a width of 20 microns (Figure 5). After photolithography, the height of the channels was spun to produce a height of 30 microns.

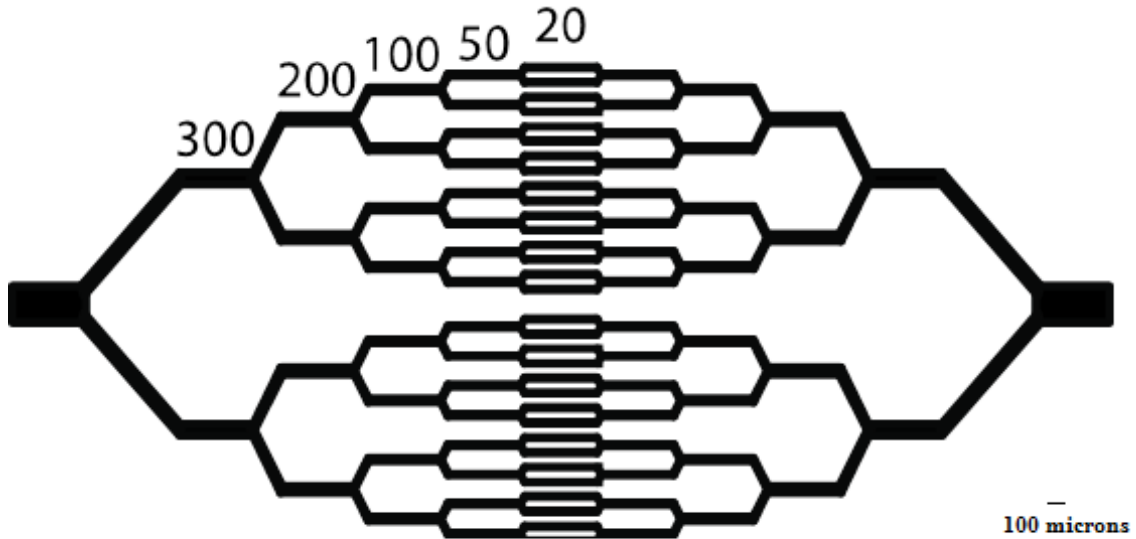


Figure 5: Model of the device used in this study. The scale bar at the lower right represents 100 μm . The numbers on top of each set of channels represents the channel width for each set. The distance from inlet to outlet is 3 cm, which represents a long microvasculature for *in vitro* studies. Each individual channel has a length of 0.4 cm.

To prepare the device, the pattern was designed by Autocad. A photomask was obtained (Photo Sciences; Torrance, CA, USA) with the pattern printed onto it. This pattern was then imprinted upon a silicon wafer (University Wafer; Boston, MA, USA) using photolithography. SU-8 10 (Microchem; Newton, MA, USA) was spun onto silicon wafers for 30 seconds using a developer hood and spin coat setup (Headway Research Model PWM32, R790 Bowl, PS Motor Assembly; Garland, TX, USA), with a starting speed of 500 RPM for 5 seconds and then ramped to 1000RPM for 20 seconds (necessary for the pattern height to be 30 microns). The wafer was then subject to a pre-exposure bake on a hot plate for 3 minutes at 65C and 7 minutes at 95C. This generated an initial layer height of approximately 30 microns on the silicon wafer. Next, the wafer was subject to UV exposure (Front-Side mask aligner in SMIF; Duke University, Durham, NC, USA) with the photomask inserted in between the UV-to-wafer path. This allowed UV exposure to crosslink the channel pattern onto the SU-8 surface. Afterwards, the wafer was subject to a post-exposure bake on a hot plate for 1 minute at 65C and 3 minutes at 95C. Finally, the wafer was soaked in SU-8 developer (Microchem; Newton, MA, USA) for 5 minutes to remove the uncross-linked SU-8 surrounding the pattern from the wafer, leaving a 30 micron-tall cross-linked pattern etched on top of a clean wafer surface.

Silanization of the silicon wafer and petri dish

Two empty and uncapped petri dishes (sterility negligible, but devoid of external particles or dust) were placed in a fume hood. A clean etched silicon wafer from the procedure above was placed in the first dish and 4-5 drops of tridecafloro-1,1,2,2-tetrahydrooctyl)-1-trichlorosilane (UCT Specialties; Bristol, PA, USA) was placed in the second dish. These dishes were then placed into a vacuum desiccator, upon which vacuum flow was turned until the system reached equilibrium. The vacuum was then turned off and the desiccator sealed off so that the silane could deposit onto

the silicon wafer while under a vacuum environment. The dessicator remained in vacuum for roughly 30 minutes, after which it was unsealed and allowed to equilibrate back to atmospheric conditions.

Preparation of PDMS Molds

Approximately 30 grams of Sylgard 184 PDMS (Dow Corning; Midland, MI, USA) was weighed out using a weighing boat and a tared weighing system. 3 ml of PDMS curing solution (a 10:1 ratio of PDMS to curing solution) (Dow Corning; Midland, MI, USA) was added to the PDMS and stirred sufficiently (but not over-stirred such that air bubbles would be present in large quantities). The PDMS solution was then poured into the silanized petri dish and on top of the silicon wafer. Afterwards, the system was placed into a vacuum desiccator and vacuumed for two hours. Any residual bubbles or particles that remained on the surface afterwards were pushed aside and dissipated using a scalpel blade.

The PDMS mold and petri dish were then placed uncovered into an oven and baked for 3 hours at 65C. Alternatively, the system could be left covered at room temperature for two days. Both of these methods allow the PDMS to fully cure, provide ample conditions for its particles to crosslink, and to ultimately harden into a rubber-like material. Higher bake temperatures were not used as we noticed they caused the PDMS surface to undulate and adopt an uneven composition after cooling down.

PDMS Removal from Petri Dish and Post-Processing

A scalpel was used to pry the PDMS loose from the edges of the petri dish. After the entire surrounding edge was loosened from the PDMS, the PDMS was peeled directly off the petri dish.

Because PDMS infiltrated beneath the wafer during the curing process, a thin layer of PDMS covered the outer surface of the wafer (facing away from the main PDMS slab). In order to

remove this layer and remove the silicon wafer from the PDMS slab, a scalpel was used to remove the edges connecting the thin PDMS film with the main PDMS slab. The thin film was peeled off the back surface of the wafer and the bulk PDMS was peeled from the front side of the wafer.

Next, a razor blade was used to slice into the PDMS such that template-etched portion of the PDMS was cut out from the rest of the slab. Each cut was done in one firm, swift motion. Cuts in which the blade was moved back and forth or up and down were avoided due to an increased risk of cracking and damaging the PDMS.

Finally, holes were punched into the inlet and outlet areas of the PDMS using an 18 gauge blunt-ended needle. The PDMS was cleaned by taking scotch tape, applying it to the surfaces of the PDMS, and then peeling it away. Figure 6 below highlights the difference between a blunt-ended needle and a sharp needle, as well as the punching technique used to obtain optimal results.

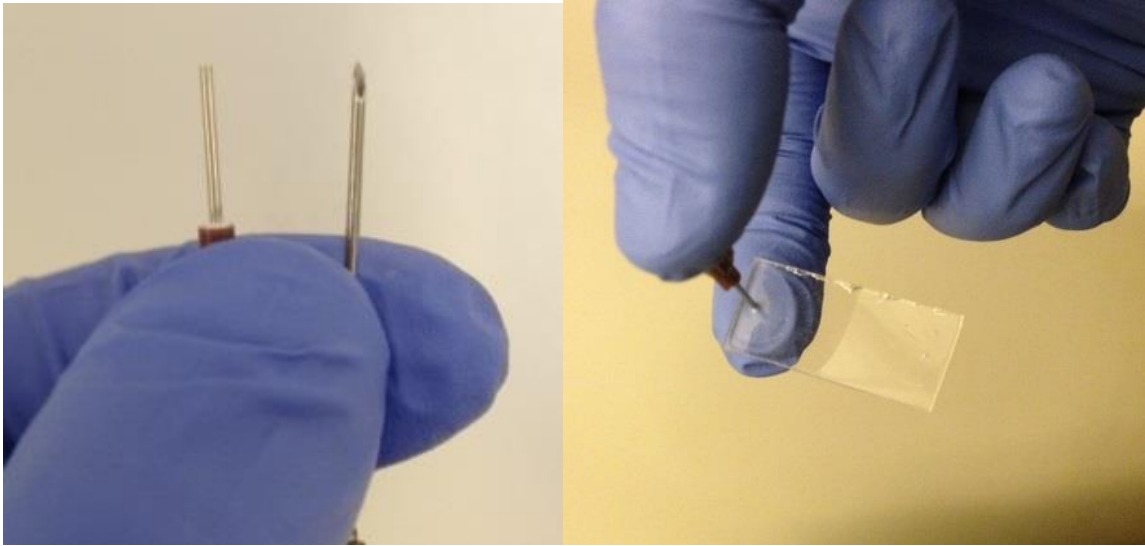


Figure 6: Punching holes through device. (Left)- The blunt-end version of a 19 gauge needle is shown on the left and the sharp-end (regular) version of the needle is shown on the right. The blunt version is used for punching holes through PDMS, while the sharp version is used to insert into tubing to act as an intermediary between syringes and tubing (Figure 8 in the Device Seeding section). *This step must be done with care because using a sharp needle to punch holes through PDMS will rip the PDMS surface and make the inlet/outlet unusable.* (Right)- Hole punching technique used to accurately punch holes through PDMS. The blunt end of the needle is lined up with the inlet/outlet, and pressure is applied on the end of the needle by the thumb while the index finger secures the back side of the PDMS

to prevent slipping. The hole is punched in one firm motion, with enough force applied so that the puncher comes out the opposite end of the PDMS and contacts the index finger. The cylindrical segment of PDMS that is punched out will stick out of the end of the needle. It is critical to remove this portion before pulling the needle backwards, otherwise the segment may get stuck back inside the PDMS slab.

Bonding the PDMS to glass slides using plasma bonding

Sonicated glass slides were placed into a plasma asher (Emitech/Quorum Technologies K-1050X; East Sussex, United Kingdom) along with the processed PDMS piece from above. The PDMS was placed so that the patterned side was facing up. The asher was run from 19 seconds at 40 watts. Immediately after the procedure, the PDMS was placed directly onto the glass slide (with the patterned side facing towards the glass) and gently pressed around all areas. The apparatus was then placed onto a heating pad at 70C for 5 minutes to ensure strong bonding (Figure 7).

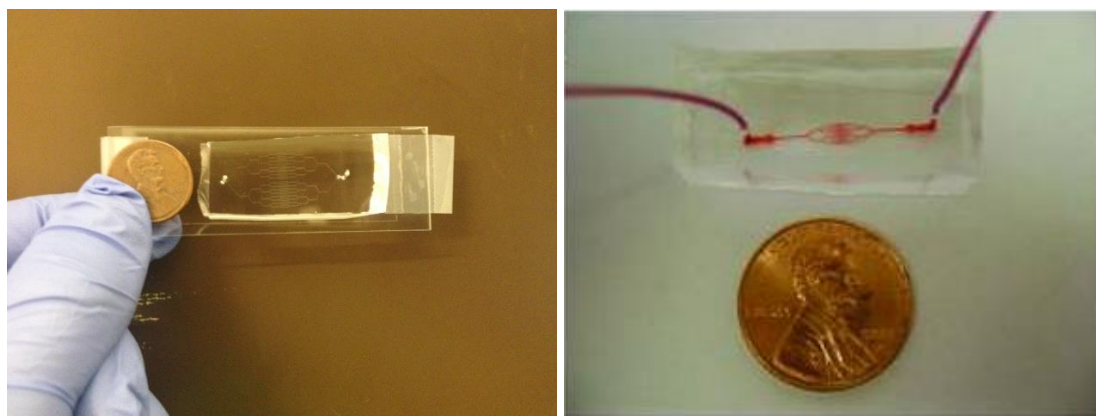


Figure 7: Bonded Microfluidic Devices. The device used in this study (left) contains very long channels, with the entire network surpassing the diameter of a standard penny. It is fabricated on a #2 coverslip, which is taped to a glass slide for mechanical reinforcement when operating on the device. In contrast, the device used in Myers et al. and Tsai et al. (right) is much smaller and is also shown next to a standard penny ^{11, 12}.

In some cases, the bonding was incomplete after a single run with the plasma asher. In these cases, folded scotch tape was placed between incompletely bonded areas to open up gaps inside the device for more exposure (Figure 8). Afterwards, the power was increased to 80 watts and the device was placed into the plasma asher again and exposed for 20 seconds. Then the incompletely bonded areas were then pressed down on again and placed onto the heating pad for 5 minutes. This cycle was repeated until all areas were fully bonded.

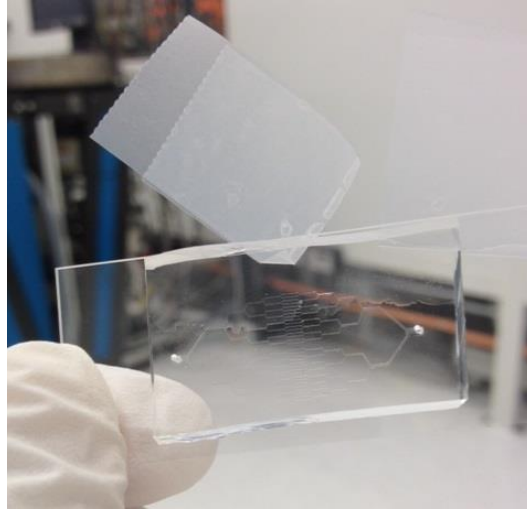


Figure 8: Folded scotch tape inserted into incompletely bonded device. The tape is folded so that the non-adhesive ends face outwards. This is placed into the device to open up the gap inside the device for better re-exposure to the asher. It is critical that no adhesive side of the tape touches the inner surface of the device.

2.2- Seeding the Device with Endothelial Cells

The device was seeded using the “Variable Flow” technique developed in this study. The following is a list of all of the individual steps necessary to accomplish successful seeding a device with microvascular channel networks.

Isolation of Endothelial Cells

In this study, human endothelial cells derived from umbilical cord blood (hCB-ECs) were isolated as described by Cheung et al.²², using the methods described by Ingram et al.¹⁵. For isolation of hCB-ECs, umbilical cord blood was obtained from the Carolina Cord Blood Bank and all patient identifiers were removed. Our lab has previously characterized hCB-ECs and found that they expressed von Willebrand factor, CD31 and VE-cadherin²³. Following exposure to 15 dyne/cm² for 24 or 48 hours, hCB-ECs aligned with the direction of flow^{23,24}, which caused them to express increased nitric oxide production and increased mRNA for endothelial cell specific genes sensitive to flow, Kruppel-like factor 2, nitric oxide synthase III, cyclo-oxygenase 2, and thrombomodulin²³.

2.2.1- Myers et al. Protocol for Seeding Microchannels

The Myers et al. protocol was used during our initial attempts to seed the microfluidic device constructed in Section 2.1. This section summarizes the general protocol that was published¹² and notes key differences between the “variable flow” protocol that was successfully used in this study and the Myers et al. protocol.

Protocol Summary

- A. The microfluidic device was pre-treated with fibronectin to help with attachment. This was accomplished through the following steps:
 1. Fibronectin (50 micrograms/ml with PBS) was flowed into the channels that had been treated with the plasma asher and allowed to cover all the channels.
 2. A 100 microliter bubble of fibronectin solution was left at the outlet to ensure that the channels stayed wet.
 3. The device was then placed into an incubator (37 degrees Celsius) for one hour.This causes the PDMS and glass portions of the channel to have fibronectin attached to them, making them attract cells at higher affinity levels.
- B. Cells were prepared at a density between 500,000 cells/ml to 1,500,000 cells/ml. Dextran 500 was added at 8% weight to volume ratio. For our studies, we used Dextran 100 between concentrations of 8-20% weight to volume ratio. Dextran 500 at 8% concentration increases viscosity by a factor of 20, while Dextran 100 at 8-20% increases viscosity by a factor of 10-80²⁵. Thus, our usage of Dextran 100 also covered the important viscosity effects of Dextran 500 indicated by Myers et al.¹². During the process of adding Dextran, it is worth noting that the infusion solution was separated into 3 aliquots and dextran was slowly added to each aliquot and thoroughly mixed.

Afterwards, the mixed aliquots were recombined to make the final infusion solution. This was done to aid the mixing of dextran, as it has a tendency to clump near-irreversibly within liquid when added in large quantities.

- C. These cells were placed into a syringe which was connected to the device inlet through connective tubing. Connective tubing at the outlet led into a petri dish for disposal of fluid that exist the device.
- D. The syringe was connected to a standard syringe pump that outputs a constant fill rate into the device. The device itself was placed into an incubator to ensure proper temperatures for attachment.

During the entire seeding process, cells would ideally be pumped into device at shear rates that would be lower than physiological values in order to ensure attachment.

- E. Media was then pumped into the device at a flow rate to maintain physiological shear rates for cells in the smallest channels. Cells would then differentiate and spread to cover any parts of the channels that they did not initially cover

Differences from the “Variable Flow” Protocol Developed in this Study

The protocol developed in this study incorporates a “Variable Flow” process. This method utilizes high cell concentration solutions that are flowed into devices. It requires the user to observe the flow-in process of cells under a microscope. The cells, regardless of density, flowed into the device in clusters which were extremely likely to aggregate at channel junctions and clog flow. Thus, flow speeds were altered dynamically: they are increased in order to unclog channel junctions and then decreased to allow sufficient cell attachment to channel surfaces. In addition, we explored the effects of the key ingredient from the Myers protocol: dextran, and ultimately decided to omit the use of dextran. Finally, we performed studies on the trypsin concentration

(ranging from 0.025% to 0.15%) used to detach the cells from their native T75 flasks while preparing the infusion solution, as this was found to have a great effect on both cell clustering and cell adhesivity to channels during seeding.

Part A from the Myers et al. ^{11, 12} protocol remains relatively unchanged in this new method, except that the concentration of fibronectin was increased from 50 micrograms/mL to 80 micrograms/mL. We found that a higher concentration of fibronectin increases the likelihood that cells would seed within the 20 micron channels.

Part B, however, was drastically different. The cell concentrations used in this method were much higher, with the lowest concentration being 3,500,000 cells/mL. We utilized experiments both with and without dextran in order to measure its effect on cell infusion. In addition, we performed trials with differing trypsin concentrations (0.025% to 0.15%) used to detach the cells during initial preparation.

Part C had one addition: A magnetic stir bar was placed within the syringe to allow sufficient mixing of the cells during infusion.

Part D was changed so that the flow was conducted while the device was under a microscope. This allows the user to view the seeding and attachment process as it happens

Part E and onwards was removed and replaced with a “variable flow” method that varies for each experiment. Even across identical cell concentrations, some seeding conditions clogged easier than others (depending on the passage # of the cells and simple random chance) and required faster flow speeds, while others contained more uniform infusion solutions and could be run at lower speeds.

2.2.2- Variable Flow Protocol

Needle and Tubing Setup

Within a sterile biological hood, a 19 gauge sharp end precision glide needle (BD; Franklin Lakes, NJ, USA) was connected to 5 inches of Intramedic PE-60 tubing (BD; Sparks, MD, USA) by having the needle inserted snugly into one end of the tubing (Figure 9). Later on, this allows the needle to be attached onto the end of a luer-lock syringe and serve as an intermediary connector between syringe and tubing. This 5 inch tubing connection was used later on for inserting fibronectin solution into the device.

This step was then repeated twice. One repeat used a 14 inch length of tubing for use during cell infusion. The other repeat used a 30 inch length of tubing for the outlet for use during device development, which allowed for the device to remain inside an incubator while being connected to a syringe pump outside.

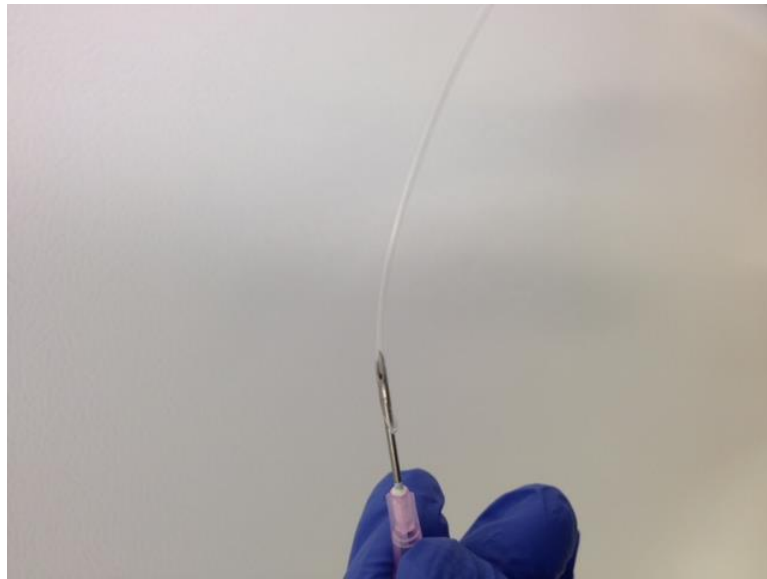


Figure 9: PE 60 tubing connected to a sharp 19 gauge needle.

Coating the channels of the device with fibronectin

The microfluidic device was pre-treated with fibronectin to help with attachment. This was accomplished through the following steps:

1. Fibronectin (80 micrograms/ml with PBS) (Sigma; St. Louis, MO, USA) was prepared in a sterile biological hood. A 1cc syringe (BD) was used to extract its contents. A needle with 5 inches of tube length was screwed onto the end of the syringe, and the other end of the tubing was inserted into the inlet of the microfluidic device.

Air bubbles that may disrupt liquid infusion were prevented from entering the device by exerting force onto the syringe while the open end of the tubing was held at a significantly higher elevation than the syringe (Figure 10). This allowed for air to be eliminated at the end of the tubing while the tubing was subjected to high gravity-driven outlet resistance, making any subsequent lowering of the height differential between the tube opening and the syringe to cause solution to flow further outwards and eliminate residual air bubbles.

Next, the open end of the tubing was inserted into the device inlet while gradually lowering the tubing end and the device as the tubing was inserted. This helped to excrete out any remaining air bubbles away from the main stream of liquid and make sure that no bubbles were trapped in between the injection stream. This procedure was repeated for every subsequent process of connecting tubing to a device, and ensured the device was free of air bubbles, especially during infusion processes in which the syringe is placed higher than the device.

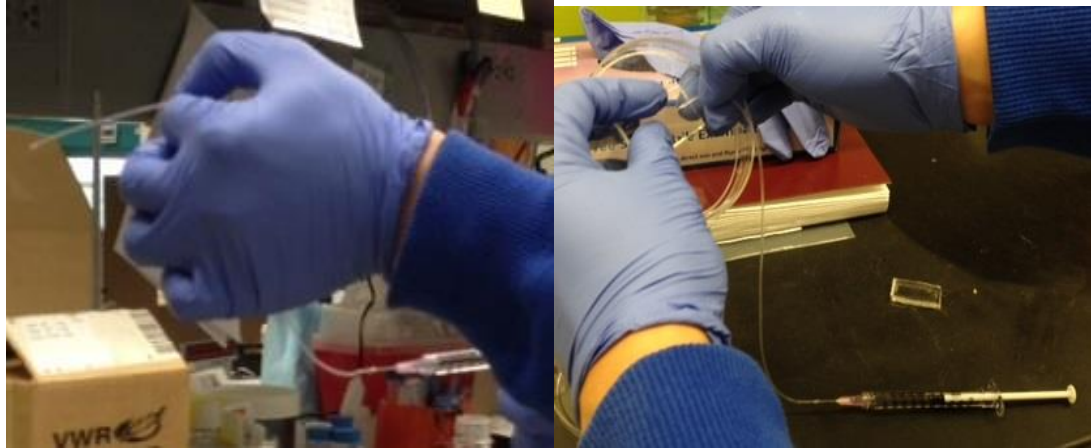


Figure 10: Elimination of air bubbles while connecting tubing to a device. (Left)- The open end of the tubing is held at a higher elevation than the syringe. The syringe is then compressed to squeeze liquid out of the end, eliminating any air bubbles during the process. (Right)- The tubing is connected to a device while the open end of the tubing is at the same elevation or lower. This causes no air bubbles to be created during the insertion process. Gradually lowering the device while connecting also assists with avoiding air bubbles that may be created from any internal resistance that might result from the small channels.

2. The syringe was connected to a syringe pump (Model PHD 2000, Harvard Apparatus; Holliston, MA, USA). Fibronectin solution was pumped through the device at 20 microliters/min. Flow was allowed to develop and reach steady-state, with an aspiration pipette sucking away fluids exiting the outlet during this time. This step is necessary to ensure that flow is slow and steady within the device, allowing for fibronectin to be uniformly distributed and mechanically settle in all of the channels. Afterwards, aspiration was discontinued and a 100 microliter bubble of fibronectin solution was left at the outlet. The pump was shut off and the syringe disconnected from the pump.
3. The syringe (including needle with solution remaining inside) was placed into an incubator (37C) for 90 minutes. This caused fibronectin to adhere to the inner channel walls, enabling endothelial cells to attach with high affinity.

Cell Solution Preparation for Infusion

Endothelial cells were grown in T75 culture flasks using a media mixture of Endothelial Basal Media (EBM-2, Lonza Clonetics; Walkersville, MD, USA) prepared with an EGM-2 SingleQuots

kit (Lonza Clonetics) and 10% fetal bovine serum (Atlanta Biologicals; Lawrenceville, GA, USA). It is important to note that all media used in subsequent steps was prepared in this fashion. After confluence, media was aspirated out and the cells were washed twice with 10mL of calcium and magnesium free PBS (Sigma; St. Louis, MO, USA). The age of the cells that achieved the most optimal seeding ranged from 13 to 40 population doublings after initial isolation. The importance of cell age and corresponding cell volume is examined in the Results section.

Next, the second wash of PBS was aspirated out and the cells were then detached from their native T-75 culture flasks using trypsin (Sigma; St. Louis, MO, USA) concentrations between 0.025% and 0.15% and incubated for 5 minutes at 37C. The effect of Trypsin concentration is also examined in the Results section. Afterwards, 8 mL of EBM-2 media was added to the flask and the cells were mixed thoroughly by pipetting the solution up and down with caution taken not to pipette too vigorously and create excess bubbles.

The solution was transferred to a 10 mL centrifuge tube and centrifuged at 1400 rpm for 5 minutes. The media was then aspirated, leaving a cell pellet. Fresh media with 10% fetal bovine serum was added to the cell palette to re-suspend the cells at a density between 3,500,000 cells/mL to 8,000,000 cells/mL and quench any remaining trypsin.

In some trials, the effect of Dextran was tested on the cell seeding process as it was indicated to be critical for obtaining positive results by Myers et al. and Tsai et al.^{11, 12}. Dextran 100 (Fisher Scientific; Fair Lawn, NJ, USA) was used to create concentrations of 8-20% weight/volume (the effects of which are documented in the Results section) with the resulting cell media mixture. In order to add and mix Dextran effectively, the infusion solution was separated into 3 aliquots and dextran was slowly added to each aliquot and thoroughly mixed. Afterwards, the mixed aliquots

were recombined to make the final infusion solution. This process was done to combat the tendency of Dextran to clump near-irreversibly within liquid when added in large quantities.

A magnetic stir bar (VWR 5x2MM Spinbar; Radnor, PA, USA), was placed into a 1cc syringe (BD; Franklin Lakes, NJ, USA) (Figure 11). The syringe diameter was just big enough to allow full rotation of the stir bar inside and generate maximum stirring effect on the infusion solution. The cell solution from above was extracted into this syringe. The 19 gauge needle and 14 inch tubing connection made earlier was retrieved and the needle was screwed onto the end of the syringe.



Figure 11: 5x2mm magnetic stir bar inside a 1cc syringe.

Experimental Setup

Using the same precautions shown during the fibronectin seeding process to eliminate air bubbles, the other end of the tubing was connected into the device inlet. A separate piece of connective tubing was placed into the outlet. The other end of this tubing was fed into a petri dish for disposal of fluid that exited the device during flow.

The syringe was connected to a syringe pump that outputs a constant fill rate into the device. The microfluidic device itself was placed onto a microscope that allowed the user to view the seeding process. A magnetic field generator was placed on top of the syringe and manually moved back

and forth about the upper surface of the syringe during the infusion process to ensure sufficient stirring of the solution. The reason the stirrer could not be moved across the bottom of the syringe was because the syringe pump took up all of the volume immediately beneath the syringe. Figure 12 below depicts the overall experimental setup.

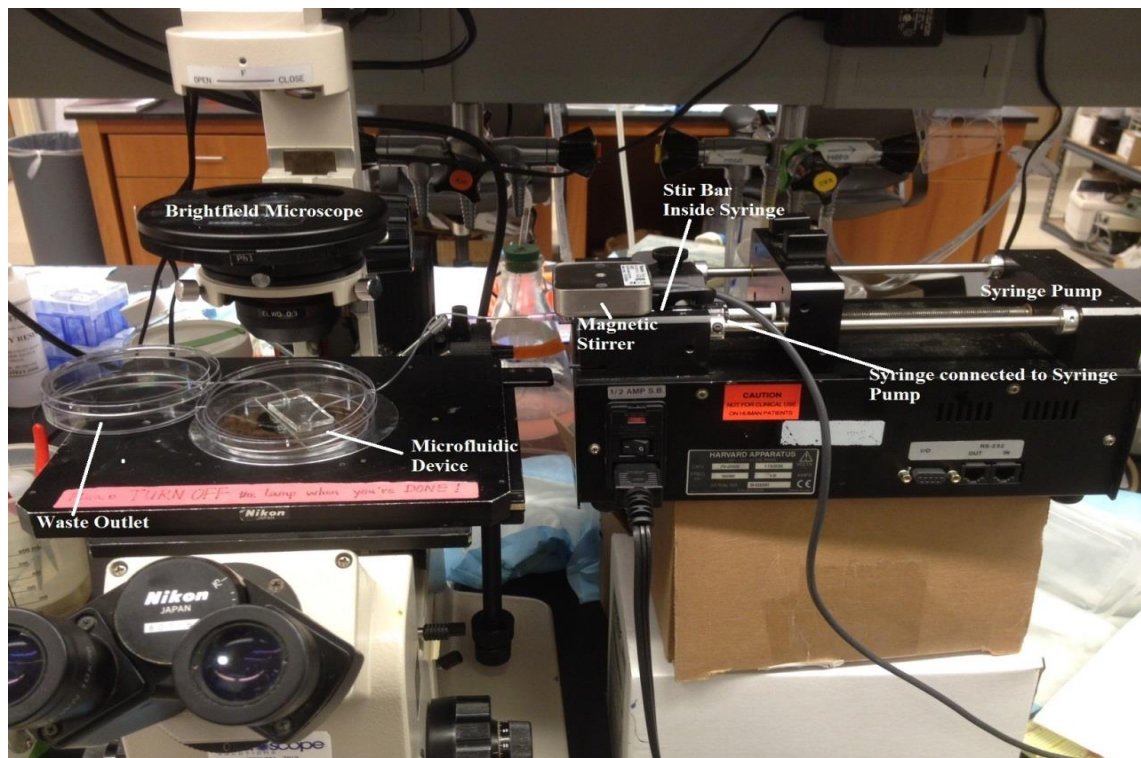


Figure 12: Experimental setup for Variable Infusion process. The apparatus is set up so that the syringe is higher than the microfluidic device, which helps cell clusters to the device with decreased resistance relative to a parallel level.

Variable Flow

This method utilizes high cell concentration solutions and variable flow rates to dislodge adherent clusters of cells. The user must observe the infusion of cells under a microscope. The cells, regardless of density, flow into the device in clusters which are extremely likely to aggregate at channel junctions and obstruct flow. These clusters were used to the advantage of seeding, as these adherent clusters in junctions could be sheared and cells could be pushed into the smallest channels by increasing the flow rate. Thus, flow speeds were altered dynamically: they are

increased in order to detach adherent clusters channel junctions and then decreased once the obstruction was removed to allow sufficient cell attachment to channel surfaces.

Given the variability when the clusters attach, the specific flow rate adjustments differ for every device. Even if the conditions used to prepare two devices are kept constant, the actual flow rates process for the devices may be different. Thus, it is possible to quantify the flow rates required for cell attachment and unclogging for specific conditions in terms of ranges, but not exact values.

Table 1 below highlights these ranges.

Table 1: Variable flow rates for differing cell ages and cell concentrations. Younger cells occupy smaller volume (see “Effects of Cell Age on Seeding” in Results section), which makes attachment slightly more difficult. This is shown in the higher flow rates needed for younger cells as opposed to older cells for attachment. In contrast, younger cells clog and unclog easier, which is why the flow rates needed for unclogging are generally smaller for younger cells than for older cells. As cell concentration increases for both young and old cells, the flow rates needed for attachment and unclogging decrease.

	Young cells (0-40 population doublings after thawing; confluent T75 flask generating over 3.5-4 million cells per flask)		Old cells (40-150 population doublings after thawing; confluent T75 flask generating under 3.5-4 million cells per flask)	
	Flow rate for attachment	Flow rate for detaching clusters	Flow rate for attachment	Flow rate for detaching clusters
3,000,000 to 4,000,000	0-3 $\mu\text{L}/\text{min}$	10-30 $\mu\text{L}/\text{min}$	0-1 $\mu\text{L}/\text{min}$	20-40 $\mu\text{L}/\text{min}$
4,000,000 to 5,000,000	0-2 $\mu\text{L}/\text{min}$	10-25 $\mu\text{L}/\text{min}$	0-1 $\mu\text{L}/\text{min}$	10-30 $\mu\text{L}/\text{min}$
5,000,000 to 6,000,000	0-1 $\mu\text{L}/\text{min}$	< 10 $\mu\text{L}/\text{min}$	0 $\mu\text{L}/\text{min}$	10-30 $\mu\text{L}/\text{min}$
6,000,000 to 7,000,000	0-.5 $\mu\text{L}/\text{min}$	< 10 $\mu\text{L}/\text{min}$	0 $\mu\text{L}/\text{min}$	10-25 $\mu\text{L}/\text{min}$

In order to illustrate how variable flow seeding works, here is the event log for a successful seeding procedure that started with an initial cell concentration of 5 million cells/mL, without dextran, and with 0.05% trypsin used to prepare the cells.

Starting flow rate: 5 $\mu\text{L}/\text{min}$

1. (0 mins) Cells began to infuse into the device for 7 minutes. Flow reached the 100 micron channels and then stopped at the 100->50 micron junctions.

2. (10 mins) Flow rate was increased to 10 $\mu\text{L}/\text{min}$ to remove the obstruction.
New clusters flowed in at higher speeds and helped break the clogging found at the 100->50 micron junctions.
3. (20 min) The entire mass of cells (now covering just about the entirety of the larger channels leading into smallest channels) started to flow into smallest channels. Three more minutes of flow went by in order to verify that the flow rate was too high for attachment.
4. (23 min) Flow was stopped for 3 minutes. More cells attached to the smallest channels. At the end of this period, no more cells were attaching and cells began to aggregate at the junctions.
5. (26 min) Flow was started again at 10 $\mu\text{L}/\text{min}$. After a roughly 30 seconds, junctions unclogged and cell masses within the channels started to move and eventually pass through the smallest channels again. An additional 1.5 minutes was allowed to verify that this was too fast for further attachment.
6. (28 min) Flow was stopped for 3 minutes to allow additional attachment.
7. (31 min): Flow was started for 2 minutes at 10 $\mu\text{L}/\text{min}$ to break clogs that formed during the previous attachment process and to allow new cells to flow into the device.
8. (33 min) Flow was stopped for 3 minutes.
9. (36 min) Flow was started for 2 minutes at 10 $\mu\text{L}/\text{min}$.
10. (38 min) Flow was stopped for 3 minutes.
11. (41 min) Flow was started for 5 minutes at 10 $\mu\text{L}/\text{min}$. More time is required for the mass to move again.
12. (46 min) The device is taken into hood and the infusion tubing is taken out of one end and put into the other (effectively switching the inlet and outlet). This allowed more

cells to cover any areas on the opposite end of the device that it couldn't cover at the original end.

13. (49 min): Flow was started again at 10 $\mu\text{L}/\text{min}$. The channels on the other end were slowly covered.

14. (56 min): Infusion solution ran out.

Unclogging Excess Aggregates and Development in an Incubator

After initial seeding, the device was placed into an incubator with the tubing and syringe still attached. The device was allowed to sit for 30 minutes to allow for sufficient cell attachment to the walls of the device. Afterwards, the device was taken out, the syringe was hooked up to the syringe pump, and the device was placed under a brightfield microscope for viewing. The flow rate was increased to 50-100 $\mu\text{L}/\text{min}$ in order to shear away any excess aggregates that were in the device. Aggregates at junctions were sheared away by flowing the media through the opposite end of the device. After flowing at high speeds for 5 minutes, the device was placed back into the incubator and allowed to develop via constant media flow from a syringe pump placed outside of the incubator. The flow rates we used were between 0.9-2.4 $\mu\text{L}/\text{min}$ during the developmental process, with both 0.9 and 2.4 $\mu\text{L}/\text{min}$ generating a confluent monolayer within the device. This process was allowed to occur over the course of 3-4 days. On the second day after initial seeding, the device was taken out again and excess aggregates were once again sheared away.

2.3- Calculations of Inlet Flow Rate, Shear Stress within Channels, and Reynolds Number

Inlet Flow Rate

Since the seeding process involves dynamically changing flow rates in accordance to the geometry of cell clusters and their levels of attachment or clogging, it is impossible to quantify a set of variable flow rates for infusion based on an ideal shear stress on channel walls. However,

for the process of growing cells within a device after seeding, we targeted the cells to experience as low shear stress as possible while on the cell walls. This would ideally give the cells a low-stress environment within these small channels to spread and grow. In conjunction with the protocol developed in the Tsai et al.¹² and Myers et al.¹¹ studies, we also targeted 1 dyne/cm² shear stress on the walls of the smallest channels.

For channels of finite width, the shear stress can be related to flow rate with the following equation:

$$t_w = \frac{6\mu Q}{wh^2} \left[1 - 16 \left(\frac{h}{w} \right) \sum_{n=0}^{\infty} \frac{(-1)^n \tanh((2n+1)\rho w / 2h)}{(2n+1)^3 \rho^3} \right] \quad (1)$$

Where Q is the flow rate, μ is the viscosity of fluid, w is the width of the channel, and h is the height of the channel. For a fluid viscosity of 0.0087 g/cm/s, channel width of 20 microns, and channel height of 30 microns, and a target shear of 1 dyne/cm² on the smallest channel walls, Q = 8.2 x10⁻⁷ cm³/sec. Assuming every one of the 32 smallest channels shares equal flow and add up to constitute the inlet flow rate, the inlet flow rate is 2.6 x10⁻⁵ cm³/sec or 1.5 μ L/min.

However, the presence of endothelial cells lining the walls of the smallest channels serves to reduce wall dimensions. In cases where protrusions from opposite walls protracted into the same space, the channel height at that location could be reduced to as low as 20 microns and the width could be reduced to as low as 10. Assuming roughly a 33% reduction in volume due to cell occupation, a 1.0 μ L/min infusion rate for growth we used corresponds to a shear stress of 1.0 dynes/cm² on the walls of the smallest channels.

What is worth noting is that the calculations from Tsai et al.¹² and Myers et al.¹¹ indicate that a flow rate of 1.23 μ L/min is needed to generate a shear of 1 dyne/cm² on their smallest channels,

which are 30 microns x 30 microns, although they did not specify the viscosity of their culture media with dextran. However, we were unable to obtain this value when attempting to implement their protocol. The flow values we obtained for their setup are: 0.9931 $\mu\text{L}/\text{min}$ without the correction factor and 1.842 $\mu\text{L}/\text{min}$ with the correction factor for a standard 0.0087 g/cm/s viscosity of media. Assuming 8% Dextran 500 increases the viscosity by twenty-fold²⁵, these flow values decrease by twenty-fold and still do not match a 1.23 $\mu\text{L}/\text{min}$ inlet flow rate.

Ultimately, we were unable to obtain uniform coverage or consistent cell attachment in long microvascular channels with their method, regardless of the flow rate used. Images from our efforts to reproduce their protocol are shown in the Results section.

Shear Stresses for Varying Flow

Table 2 shows the shear stress on channel walls for varying flow rates, some of which were used within the “variable flow” protocol during cell attachment. They are computed using Equation 1. No Dextran is used within the media for these calculations and the viscosity is set at 0.0087 g/cm/s. As the flow rate increases, the shear stress on the channel walls increases, which serves to aid the detachment of clusters on the walls. The shear stress experienced within a channel also increases with channel size, which also follows our findings during the steps of de-clogging aggregates. Cell aggregates from upstream flow tend to flow into downstream aggregates first before the downstream aggregates are then cleared, signaling higher shear stress experienced in upstream channels.

Table 2: Shear stresses experienced on 20, 50, and 100 micron channel walls with respect to varying inlet flow rates. No Dextran is present within the infusion media.

	Shear stress in channel walls for 1 microliter per min inlet flow (dynes/cm ²)	Shear stress in channel walls for 5 microliter per min inlet flow (dynes/cm ²)	Shear stress in channel walls for 15 microliter per min inlet flow (dynes/cm ²)	Shear stress in channel walls for 25 microliter per min inlet flow (dynes/cm ²)	Shear stress in channel walls for 40 microliter per min inlet flow (dynes/cm ²)
20 µm channel	0.63	3.16	9.49	15.82	25.31
50 µm channel	0.82	4.11	12.33	20.54	32.87
100 µm channel	1.03	5.14	15.41	25.69	41.08

Table 3 shows the effect of adding Dextran into the infusion media on the shear stress experienced within channel walls. Dextran 500 at 8% (or Dextran 100 at 15%) causes a viscosity increase by a factor of twenty ²⁵, so the fluid viscosity used for these experiments is $0.0087 \times 20 = .174$ g/cm/s. The high shear stress values also explain why during our attempts to utilize dextran with our “variable flow” technique, we needed to use a much lower flow rate (Section 3.6).

Table 3: Shear stresses experienced on 20, 50, and 100 micron channel walls with respect to varying inlet flow rates. Dextran is present within the infusion media.

	Shear stress in channel walls for 1 microliter per min inlet flow (dynes/cm ²)	Shear stress in channel walls for 5 microliter per min inlet flow (dynes/cm ²)	Shear stress in channel walls for 15 microliter per min inlet flow (dynes/cm ²)	Shear stress in channel walls for 25 microliter per min inlet flow (dynes/cm ²)	Shear stress in channel walls for 40 microliter per min inlet flow (dynes/cm ²)
20 µm channel	12.66	63.29	189.86	316.43	506.29
50 µm channel	16.43	82.12	246.5	410.83	657.33
100 µm channel	20.54	102.71	308.13	513.14	821.67

Reynolds Number within Channels

The Reynolds number within channels was calculated for 20, 50, and 100 micron wide channels using the following equation:

$$Re = \frac{\rho \langle v \rangle D_h}{\mu} = \frac{\rho \langle v \rangle 2wh}{\mu(w+h)} \quad (2)$$

Where ρ is the fluid density, $\langle v \rangle$ is the average velocity of fluid within the channel, μ is the fluid viscosity, D_h is the hydraulic diameter of the channel, w is the width of the channel, and h is the height of the channel. No Dextran is used to affect the viscosity of media within these calculations. The results for the channels are shown below in Table 4.

Table 4: Reynolds number for 20, 50, and 100 micron channels with respect to varying inlet flow rates. No Dextran is present in the media for these calculations.

	Reynolds Number in channel for 1 microliter per min inlet flow	Reynolds Number in channel for 5 microliter per min inlet flow	Reynolds Number in channel for 15 microliter per min inlet flow	Reynolds Number in channel for 25 microliter per min inlet flow	Reynolds Number in channel for 40 microliter per min inlet flow
20 μm channel	0.025	0.12	0.36	0.60	0.966
50 μm channel	0.030	0.15	0.45	0.75	1.20
100 μm channel	0.037	0.18	0.55	0.92	1.47

The Reynolds number increases as the channel size increases, and the differential between the Reynolds numbers also increases as flow rate is increased. Although still small, the values in Table 4 signify that inertial forces are slightly more prevalent within larger channels than for

smaller channels, which corresponds to our findings that cell clusters tend to attach better in larger channels than within smaller channels at low flow rates. Furthermore, this also agrees with our findings that individual cells attach better within smaller channels where inertial forces are slightly less prevalent and the channel volume is smaller (Section 3.4).

2.4- Imaging Seeded Devices

Fixing and Staining Seeded Cells

A device that was fully confluent was washed by connecting it to a syringe pump and flowing PBS into its channels for 5 minutes at 10 $\mu\text{L}/\text{min}$. Afterwards, cells inside the device were fixed by flowing 10% formalin (Azer Scientific; Morgantown, PA, USA) into the channels at 5 $\mu\text{L}/\text{min}$ for 30 minutes. Next, the device was washed again with PBS for 15 minutes. A 1% Triton X-100 solution (Sigma; St. Louis, MO, USA) was then flowed into the device at 2.5 $\mu\text{L}/\text{min}$ for 5 minutes. The cells in the device were then blocked with 3% bovine serum albumin (Sigma) that was flowed into the channels for 1 hour at 2.5 $\mu\text{L}/\text{min}$. Next, primary goat antibody (1:250 with PBS) with VE-cadherin (Santa Cruz Biotechnology; Dallas, TX, USA) targeting was flowed into the device for 2 hours at 1.5 $\mu\text{L}/\text{min}$. Finally, TRITC conjugated anti-goat IgG secondary antibody Alexa Fluor 488 (1:250 with PBS) (Invitrogen, Life Technologies; Grand Island, NY, USA), along with Hoechst 33342 nuclear staining antibody (1:2000 with PBS) (Invitrogen, Life Technologies), was flowed into the device for 1 hour at 1.5 $\mu\text{L}/\text{min}$. The device was then cleaned one final time by flowing PBS through at 10 microliters/min for 15 minutes. It is important to emphasize that great care was taken to ensure no air bubbles entered the device between each step. The method for doing this is shown in Figure 9 in the needle and tubing setup section.

Immediately after this process, both the inlet and outlet tubing were scissor-cut roughly 2-3 millimeters above the entrance ports (while still connected). This ensured that PBS remained

within the channels and a small reserve of PBS would be left within the tubing that still remained connected to the device. The device was then wrapped in tin foil for storage.

Stained devices were viewed under a 510 laser scan inverted confocal microscope (Zeiss; Jena, Germany) with both 488 (green) and 405 (blue) wavelength lasers in order to image VE-cadherin interactions (green) among cells and to visualize the location of cells within the channels via their nuclei (blue).

2.5- Sickle Blood Flow into Seeded Devices

For a detailed protocol, complete with pictures, please see Appendix B.

Fully-recessive HBSS blood was obtained from the Duke University Hospital. The blood was not diluted and white blood cells were not removed. The blood was placed along with a magnetic stir bar into a syringe. The syringe was then sealed with a luer-lock connector already fit with connective tubing. The syringe was then placed onto a syringe pump and calibrated so that the syringe was ready for flow, with the diaphragm of the machine touching the plunger of the syringe.

The syringe was then connected via connective tubing to a seeded device on one of the ports. Finally, tubing was also connected to the other device port, which led to an empty petri dish to serve as outlet waste disposal. The entire system was then placed next to a microscope with video recording capabilities in order to visualize the flow. A magnetic stirrer was placed on top of the syringe in order to prevent cells from settling during the flow process

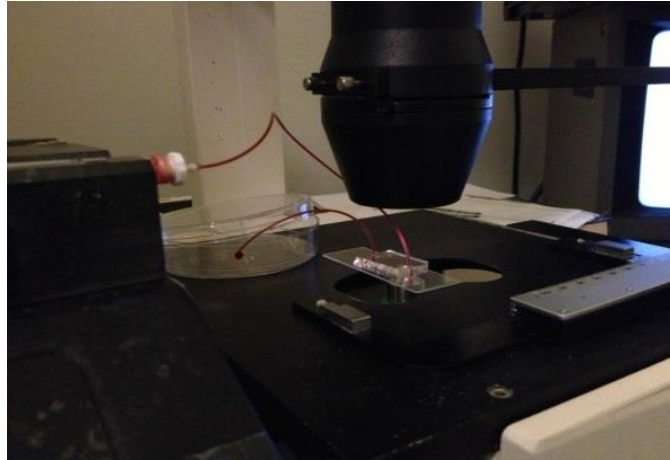


Figure 13: Flow experiment being conducted and recorded on a microfluidic device.

Blood was then flowed through the device at a starting speed of 10 $\mu\text{L}/\text{min}$ in order to get flow started within the device (Figure 13). The speed was then reduced to more physiological levels of blood flow. In most cases, 1.0-1.5 $\mu\text{L}/\text{min}$ was used in order to generate minimal physiological shear stresses on the walls and in order to visualize the pathway that the sickle cells took without flow being too fast for analysis. Afterwards, the individual flow paths of blood within the smaller channels were analyzed and the overall effects and impacts of sickle aggregations within the device were studied.

Chapter III: RESULTS

3.1- Results Obtained Using the Myers et al. Protocol

The first step in producing endothelialized channels in long microvascular networks was to test the protocol of Myers et al.^{11, 12}. While mimicking the exact protocol outline by Myers et al.^{11, 12}, with the exception of Dextran 100 used instead of Dextran 500 (which still generated the effects of Dextran 500 as mentioned in Section 2.21), the seeding process faced multiple challenges.

They are as follows:

1. With an infusion rate of 1.23 $\mu\text{L}/\text{min}$ as indicated by the protocol, cells do not flow into the device at the same concentration as the cell solution within the syringe, which is noted to be anywhere between 500,000 cells/ml to 1,500,000 cells/ml¹². Cells tend to aggregate and settle inside the syringe, regardless of whether or not dextran is used in the solution. Furthermore, trypsin concentrations of 0.025% and 0.05% indicated no changes in seeding coverage of the channels and did not seem to significantly impact cell entry into the syringe.
2. Cells entering the device were present as aggregates and individual cells. These aggregates could have formed due to the time taken for cells to infuse into the channel.
3. Clogging by the aggregates generally occurs in small channels, as shown in Figure 14 below. This is especially prevalent for channels with dimensions of 20-30 microns or lower. It is important to note that clogging occurs for all cell concentrations examined, ranging from 500,000 cells/ml to 1,500,000 million cells/ml.

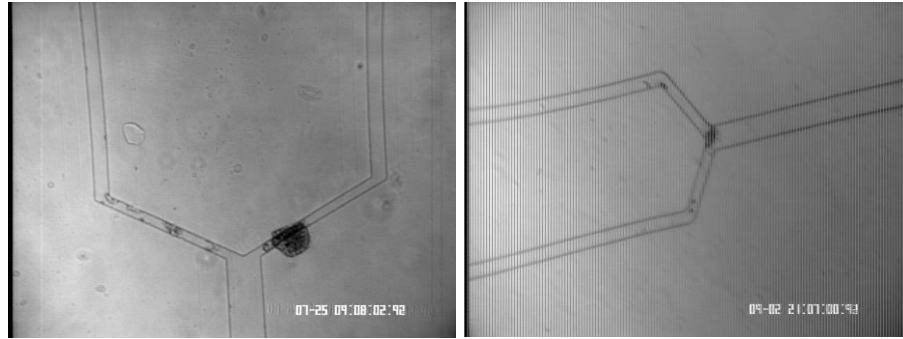


Figure 14: Clogging in channel of 20 microns x 30 microns dimensions. The picture on the left depicts clogging and subsequent leakage for 500,000 cells/ml, and the picture on the right depicts clogging for 1,500,000 cells/ml. Clogging occurred at the junction leading into the 20 micron channel or immediately within the 20 micron channel.

4. Seeding at 0.3 $\mu\text{L}/\text{min}$ results in initial clogging within small channels and junctions leading to them. For flow rates as high as 20 $\mu\text{L}/\text{min}$, clogging by endothelial cell aggregates is very likely at the junctions leading to the 20 and 50 micron channels. However, the cell concentration is not sufficient to dislodge this initial clogging (Figure 15).

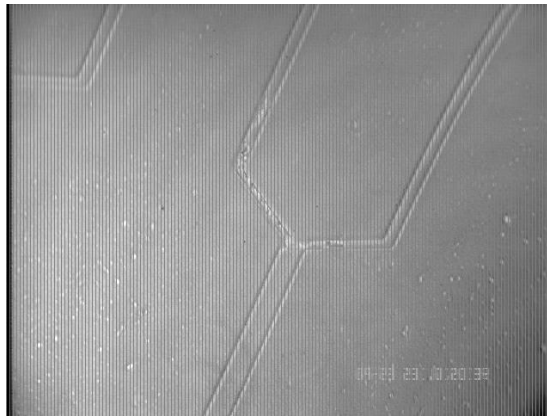


Figure 15: Clogging in channel of 20 x30 microns dimensions and 0.3 microliters/min inlet flow rate.

5. Any clogging within the smallest channels effectively stops the seeding process. Clogging at these junctions interrupts flow and greatly increases resistance for cells and

clusters to enter the device. This leaves empty channels in the larger channels after initial clogging in the smaller channels, regardless of flow speed. Figures 14 and 15 from above shows this to great effect. For example, the larger channel (50x30 microns) is completely empty after clogging in the smaller channels (20x30 microns) inhibits flow

6. Even when cell attachment occurs, cells need to be in very close proximity to each other in order to spread (Figure 16). Generally, the Myers et al. procedure will produce around 1-2 EC aggregates per channel, which do not cover enough overall area for cells to be able to proliferate and spread across the entire channel wall. Despite flowing media continuously into the device for multiple days and at physiological flow rates of 1.1 mL/min, the cells rarely spread and an endothelial layer did not form.

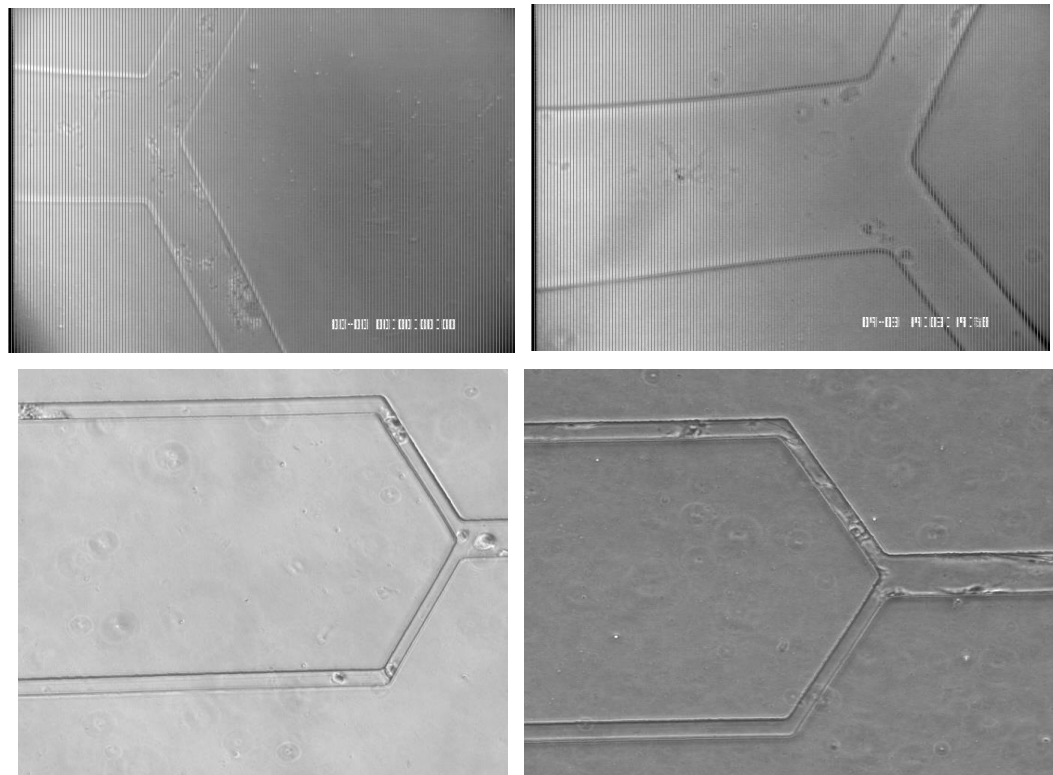


Figure 16: Amount of cell seeding within channels is insufficient to produce a monolayer. The images on the left represent the initial seed images within, while the images on the right represent the channels after two days of flowing EBM-2 media into the device at 1.1 μ L/min. The upper pair shows a 200 micron to 100 micron junction, while the bottom pair shows a 50 micron to 20 micron junction. Note that in the bottom pair, the bottom channel is virtually uncovered during seeding and no spreading cell spreading occurs during subsequent media development.

3.2- The need for “Variable Flow”

Given the results from the Myers et al. protocol ^{11, 12}, the most significant problem was due to cells not being able to flow into the device after an initial burst of flow. The problem here is twofold:

1. The cells are clustering and aggregating at the bottom of the syringe, which greatly increases their resistance against entering the inlet after an initial amount of clogging.
2. Early into the seeding process, cells enter the device as both single cells and clusters. Over time, as the trypsin is quenched by the media solution, the cells enter as increasingly large clusters. Regardless of their entry conformation, cells aggregate at channel junctions and even within the middle of smaller channels. This effect serves to increase the flow resistance and limit further cell infusion.

After an initial amount of infusion and cell attachment, these two factors greatly inhibit further entry of cells into the device. Since the viscosity of cell infusion solution is relatively low compared to other cell-rich fluids that are pumped through devices (such as blood), eventually the only matter entering the device is the base cell media due to resistance within the device and cells settling at the bottom of the syringe. Thus, the cell concentration entering the device is not nearly the same as the overall cell concentration within the syringe. This effect was especially noticeable for the Myers et al. protocol with cell concentrations of less than 1,500,000 cells/mL ¹².

As mentioned in the “variable flow” protocol, the combination of a micromixer that was placed inside the syringe and a high cell concentration (greater than 3,500,000 cells/mL) significantly helped with allowing cells to enter the device. A magnetic field generator that was moved back and forth across the syringe surface, causing the micromixer to move and stir along with the

motion, helped prevent cell settling within the syringe. The amount of cells in the solution was greater, and thus the probability of mixing and forcing cells through the tubing and into the device was also higher.

Furthermore, as the cell media quenched the trypsin surrounding the cells over time, cells began to flow into the device in clusters. The timescale for this is within minutes of re-suspending the cells in media for infusion into the device. This effectively made clogging within junctions leading to the smallest channels inevitable. In order to get around this, we hypothesized that having an extremely high cell concentration generates a greater impulse force for clearing clogged junctions within channels. Support for this proposal comes from Zhang et al.¹⁰ and Rosano et al.¹⁴ in which a density of 30,000,000 cells/mL and 10,000,000 cells/mL, respectively, was used to successfully seed a device of 100x100 micron dimensions.

However, with just a higher cell concentration and the implementation of a stir bar, seeding coverage still poor after using a constant flow rate for 2. Cell aggregates still formed in the small channel junctions and ultimately prevented further cells from flowing into the device. After initial clogging, mostly culture media was observed to flow into the channels, with the cells being left behind in the syringe or sparsely upstream due to high resistance in the channels.

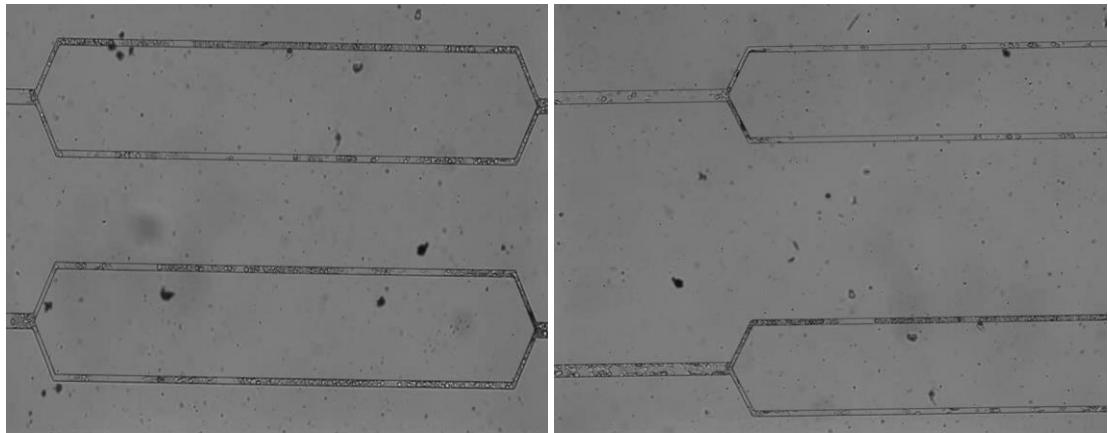
We hypothesized that the infusion rate would need to be increased periodically to dislodge cell clusters when junctions became clogged, and then decreased again to allow these clusters to attach. In particular, we noticed that an infusion rate of 5 microliters/mL tended to serve as the best starting point, and after 10 minutes this would be “dynamically” adjusted to accommodate random clogging or flow that is too fast for attachment, usually within the smallest channels. The dynamic adjustment rates can be found in Table 1 in the Section 2.22.

Thus, for our successful experiments, infusion was viewed with a brightfield microscope and flow was dynamically accelerated and stopped between a range of 1 $\mu\text{L}/\text{min}$ to 30 $\mu\text{L}/\text{min}$ based upon the level of clogging or attachment within the channels. As mentioned in the methods section, it is critical to emphasize that these rates and ranges will vary for each device, sometimes drastically so. Some initial aggregates within junctions may require as high as 30 $\mu\text{L}/\text{min}$ flow rate in order to clear, while some others will only require flow rates as low as 10 $\mu\text{L}/\text{min}$.

Although the specific pattern of variable infusion process will inevitably vary with each procedure, as the results of cluster attachment and clogging are very random, especially within channels of 20 micron diameter or smaller, it is possible to reproducibly seed channels.

3.3- Seeding Results

The “Variable flow” procedure outlined in the Methods section generated the following seeding results (5 million cells/mL infusion concentration):



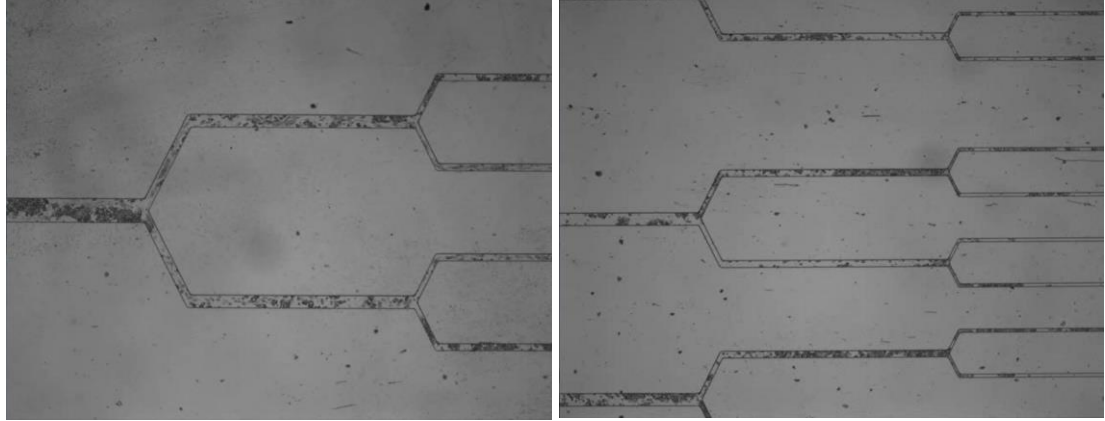
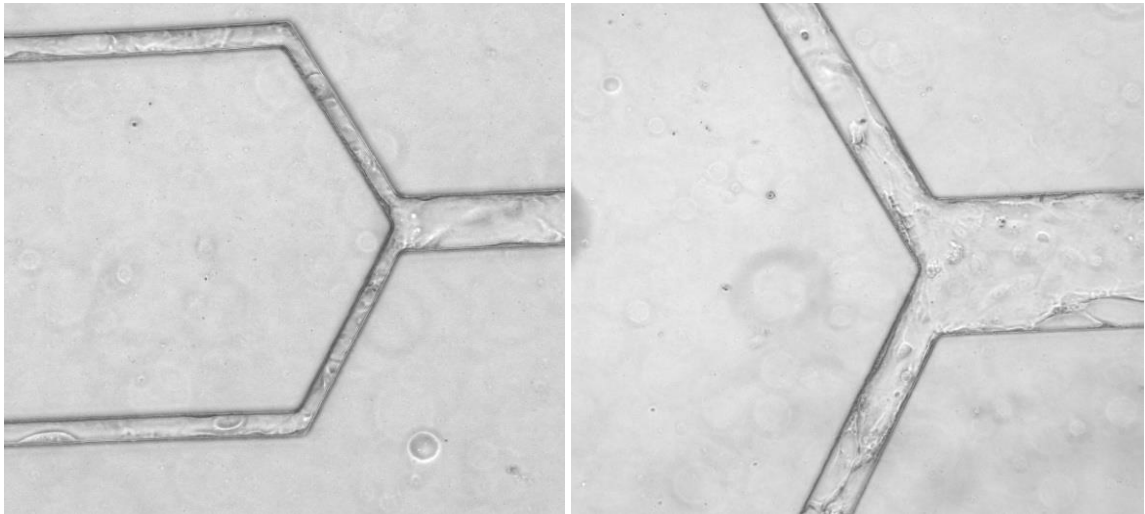


Figure 17: Initial EC seeding of channels within the device. Images were taken immediately after the “Variable flow” process ended for a seeding of 5,000,000 cells/mL. The upper panel shows channels of micron dimensions, while the lower panel shows larger channels that are of 200, 100, and 50 microns.

The entire device was seeded in the orientation shown in Figure 17. All of the channels were fully covered by an initial layer of cells except the smallest channels, which only resulted in partial coverage. For 5,000,000 cells/mL, the percent coverage of all of the smallest 20 micron-wide channels generated was roughly 60% (Figure 19). However, this was sufficient to generate confluency throughout the device after it was subject to incubation and media flow for 3 days. Signs of cell growth can be seen within the first two days, as shown below in Figure 18.



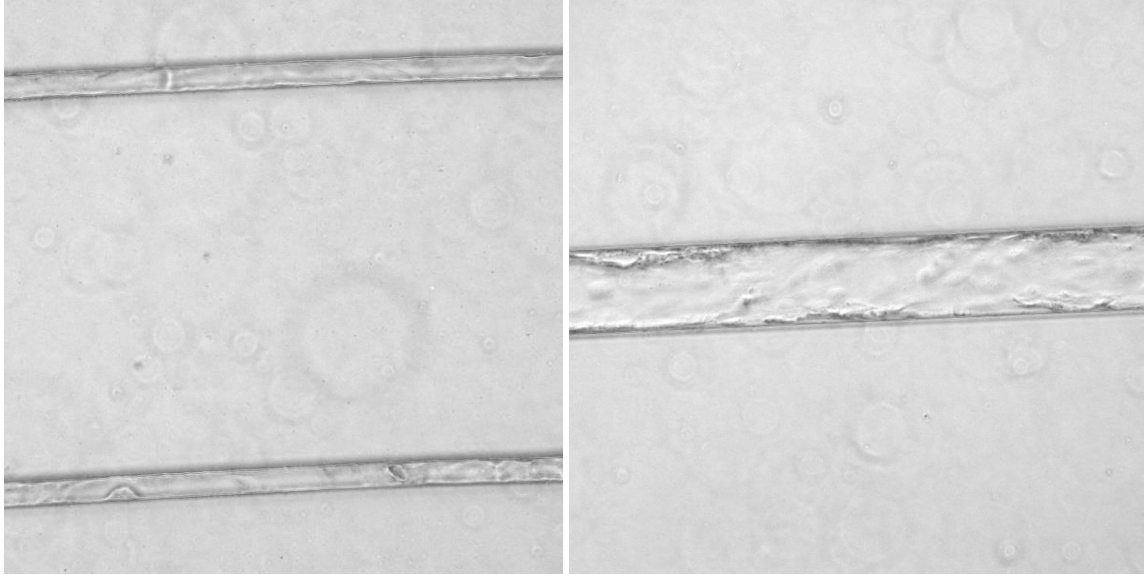


Figure 18: Early confluency within microchannels. The upper left shows cell growth within a 50 to 20 micron junction, the upper right shows cell growth in a 100 to 50 micron junction. The bottom left shows cell growth in the middle of the 20 micron channels, and the bottom right shows growth in the middle of a 50 micron channel.

Throughout our tests, the lowest percent coverage seen to generate confluency was roughly 20 percent, which meant the cells spanned past the initial junction area and into the horizontal region of the smallest channels. This corresponded to an initial infusion concentration of 3,500,000 cells/mL. Figure 19 below shows a chart mapping the correlation between percent coverage and infusion concentration.

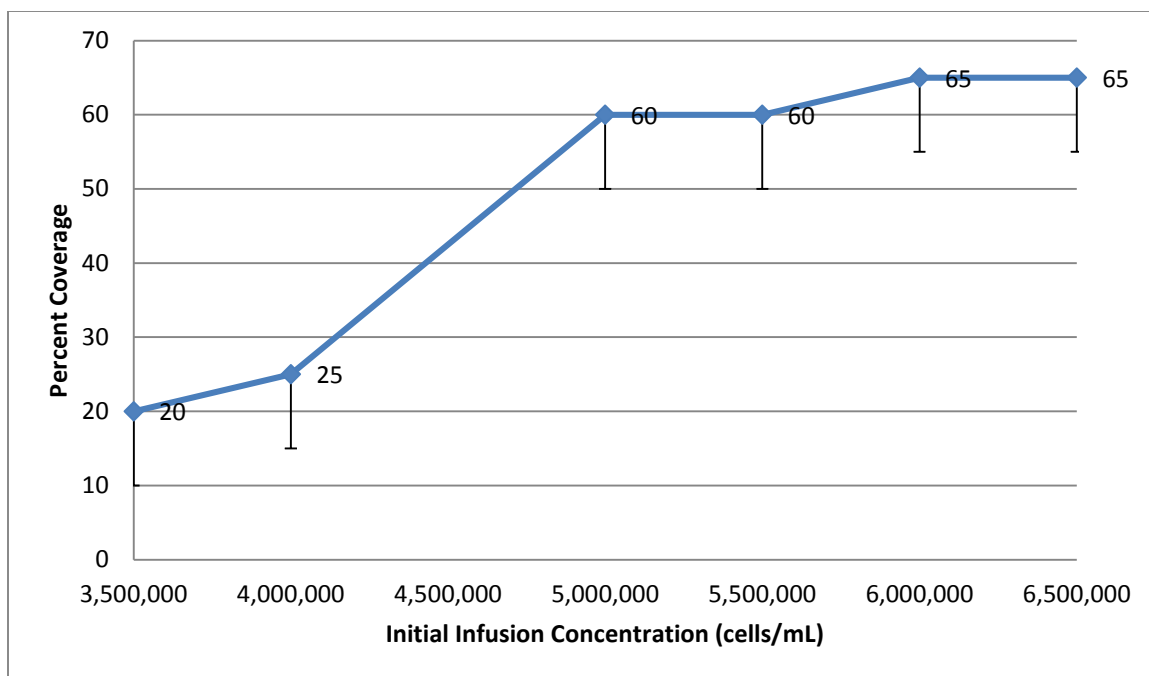


Figure 19: Percent coverage of smallest channels (20 microns) vs. initial infusion concentration of cell solution (cells/mL) for Variable seeding. The percent coverage values for each concentration, over the course of 3 trials each, fall within 10% below the listed value. The listed value is the maximum percent coverage observed for each concentration among trials conducted. The trypsin concentration used to prepare the cell solution in every case was 0.05%, with residuals using higher concentrations such as 0.1% and 0.15% showing inhibited cell attachment (see Section 3.6). Dextran 100 (8-20% weight/volume) was used in some of the 3,500,000 cells/mL and 5,000,000 cells/mL trials and showed no noticeable difference in percent coverage. These results should be consistent as long as seeding is performed properly and with cells that are no older than 5 passages after thawing (section 3.5). Each point is the approximate average of three experiments.

We observed a non-linear relationship between the concentration of cell solution and the percent coverage generated by the smallest channels. This is likely due to the random nature of clogging at junctions, the amount of cells that are lost during the “Variable flow” process of clearing these clogs, and the degree of cell towards the bottom of the syringe during infusion. Within the concentration ranges indicated, higher concentrations will likely yield a higher percent coverage of the smallest channels during initial seeding. However, the increase in percent coverage seems to flatten out at higher cell concentrations, which is consistent with previous findings from our lab depicting endothelial cells adhering to surfaces coated with fibronectin ²⁶. The reasoning behind the findings in this study is perhaps due to that increased cell concentrations eventually cause

clogging to be too intense at junctions leading to the 20 micron channels and become progressively harder to shear away as cell concentration increases.

3.4- Cell Attachment and Growth Mechanics

While conducting seeding under a brightfield microscope, we noticed that cells in clusters of 2-15 cells per cluster had a much higher chance of attaching to larger channel walls than single cells did, regardless of the flow rate. These cluster sizes can be as small as 10 microns and as big as 70 microns in diameter. For the smallest 20 micron channels, cluster sizes of 2 cells or a larger small cell were ideal for attachment. Figure 20 below shows cluster sizes for both larger channels and the smallest channels. In addition, areas that contained multiple attached clusters had increased likelihood of more clusters attaching and eventual growth during development. Occasionally, individual cells experienced difficulty in attaching to cell walls. Even the pump was stopped, individual cells tended to flow out of the channels and through the outlet of the device. In areas that contained multiple attached clusters, single cells often collided with the adherent clusters and returned to the flow without adhering.

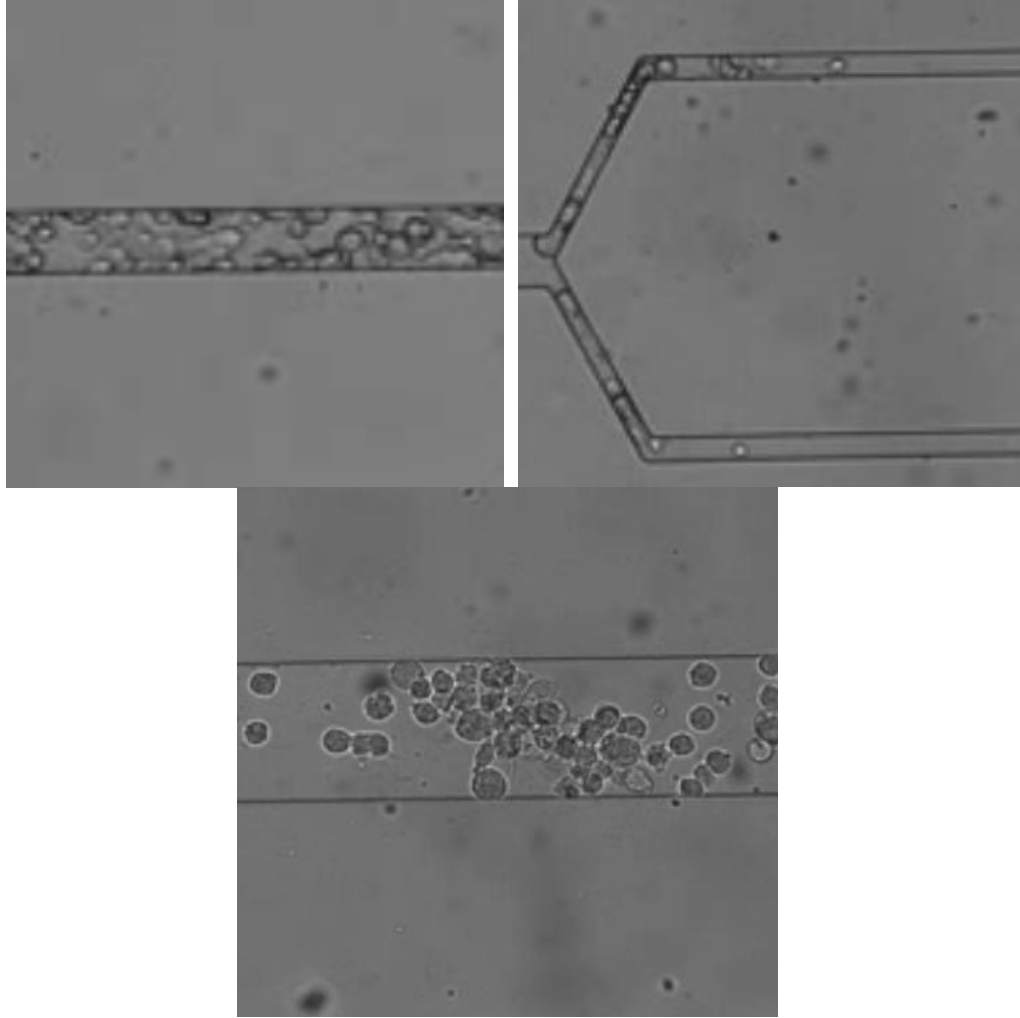


Figure 20: Cell attachment within larger and smallest channels during seeding flow. The figure on the upper left shows cells attached to the walls of a 50 micron channel. Most of the cells attach to the channel wall in clusters of 2-5 cells per cluster, while the cells in the middle are flowing through the channel. This effect was also consistent with channels of larger dimensions. The average cluster size is approximately 20 microns. The figure on the upper right shows cells attached to the walls of a 20 micron channel. The cells attached are either clusters of 2 cells or larger single cells (15-25 microns in diameter) that can deform slightly to fit into the channel. The average cluster size is between 10-20 microns. The figure on the bottom shows two clusters of 10-15 cells attached next to each other within a 100 micron channel. The average cluster size is roughly 60 microns.

Individual cells or isolated clusters that may have attached during the seeding process generally did not survive after incubation and steady media flow (1-10 $\mu\text{L}/\text{min}$) over a few days. This is shown in great detail through pictures from our results using the Myers et al. protocol^{11, 12} (Section 3.1). In contrast, variable flow seeding (Section 3.2) produced adhesion of multiple clusters that tended to grow into fully confluent layers within channels (Figures 26-29).

Thus, for larger channels, cell attachment and growth is improved when multiple clusters attach within close proximity to one another. For the smallest channels, it is ideal to have cells (whether individual or clustered) in very close contact with one another and spanning into the horizontal region of the channel (an example is shown in section 3.5). It is also possible to get a confluent monolayer to develop with individual cells attaching in close proximity to one another. The likelihood of individual cell attachment within larger channels is very small, while the likelihood of individual cells attaching within the 50 and 20 micron channels is higher. However, at lower flow rates, the likelihood of cluster attachment within larger channels is higher than in smaller channels. Both of these findings agree with our Reynolds number calculations within channels of varying sizes (Section 2.3). Finally, recorded seeding videos showed that clusters that attached seemed to be traveling at an axial velocity of 0.04 cm/s prior to attachment. They took anywhere between 0-8 seconds to settle.

3.5- Cell Concentration Values and Cell Properties- *Minimum and Maximum Concentrations Thresholds, Effects of Higher Infusion Concentrations, and Cell Age*

One of the most significant parameters of interest for seeding is the cell concentration entering the channels, a parameter which had not been addressed in published studies. Unlike the Zhang et al. ¹⁰, in which 30 million cells/mL was seeded into 100x100 micrometer channels ¹⁰, we found that it is not possible to seed extremely high cell densities into devices with channel widths ≤ 20 microns. Doing so will cause leakage to the bonding surrounding the microvascular-sized channels and perhaps leakage at the inlet port. For channels with widths ≤ 20 microns, a very specific range of cell infusion concentration may be necessary in order to ensure high success.

Minimum Cell Concentration for Seeding

After extensive testing, the minimum seeding concentration was found to be roughly 3.5 million cells/mL. During the seeding process, this was enough to push aggregates past junctions leading into the smallest channels and travel part way into the channels themselves. After being exposed to media flow for three days, these channels showed confluent cells. Concentrations below 3.5 million cells/mL did not sufficiently penetrate the smaller channels and development was unable to generate a monolayer within the 20 micron channels.

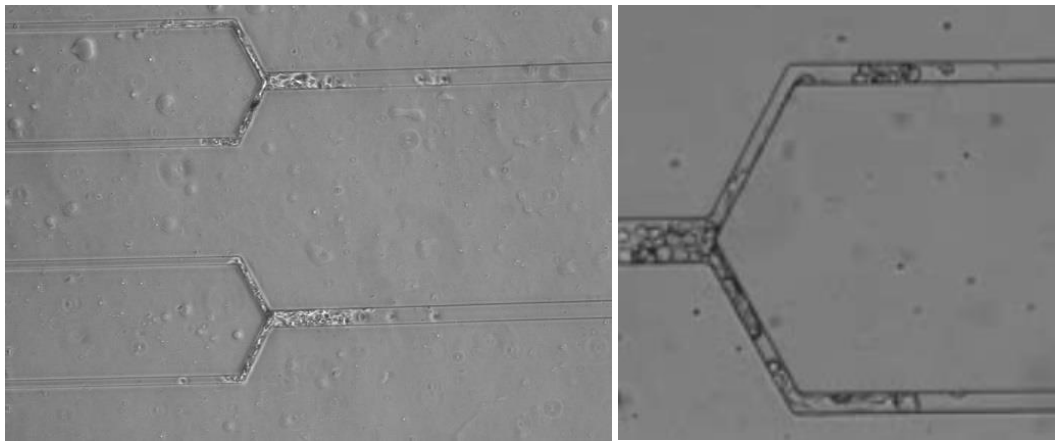


Figure 21: Initial seeding after for 3.5 million cells/mL (minimum successful concentration) within smallest channels. The cells are able push past the junction are and travel into the horizontal region of the 20 micron channels.

Threshold Concentration for Leakage

A cell concentration equal to greater than 8 million cells/mL caused channel leakage. Thus, we highly recommend using a concentration smaller than this amount for seeding devices. Two devices out of two generated very similar leakage results for concentrations of 8 million cells/mL.

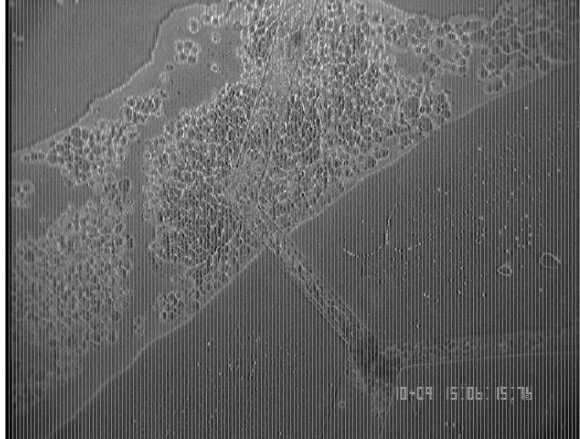


Figure 22: Threshold concentration for leakage is reached within 20 a micron channel as a result of 8 million cells/mL infusion concentration.

Effects of Higher Cell Concentrations Used for Seeding

From these test results, it can be inferred that concentrations within the range of 3,500,000 to 8,000,000 cells/mL may generate successful and safe seeding results. However, higher concentrations between 5,500,000 cells/mL and 8,000,000 cells/mL were prone to experiencing excess cell aggregates within channels of 100 micron width or larger. This resulted in entire bodies of excess cell clusters impeding flow paths within larger channels after initial seeding. For concentrations under 7,000,000 cells/mL, these bodies could mostly be sheared away under increased flow rates of EBM-2 media. This process is explained in detail in the *Unclogging Aggregates* portion of Section 2.22.

For 7,000,000 cells/mL, these aggregates were too abundant or firmly adherent and could not be sheared away by a significant amount. Some cellular membranes of the cells attached to channel walls were lysed during this process, damaging any endothelium that may have been forming at the time. Based on these results, ideal infusion concentrations should be between 3.5 million cells/mL and 5 million cells/mL.

Endothelial Cell Age

In addition to infusion concentration, cell age is perhaps one of the most important factors that contribute to successfully seeding a device. Cells that are young (no more than 1-3 passages after thawing) seemed to experience a much easier time entering the smallest channels than older cells did. However, we did not notice a significant difference in cell volume between suspended young and old cells. Despite this, our T75 flasks that were confluent with young cells (less than 4 passages or 31 population doublings after thawing) generated up to 5.5 million cells per flask, whereas our T75 flasks that were confluent with older cells (over 4 passages or 31 population doublings after thawing) only generated up to 2.8-2.9 million cells per flask. This indicates that younger cells perhaps be more deformable and can fit into tight spaces, whether it be occupational space on a flask or into smaller channels in a microfluidic device, which allows them to be seeded with more efficiency and ease during our “variable flow” process.

In our tests with younger cells, the seeding process took significantly shorter (sometimes only 10-15 minutes) than tests run with older cells (which sometimes occupied over an hour). Trials with older cells were much more prone to clogging at the junctions, which meant that more cells and an elevated infusion rate had to be used to push past these clogs. This sometimes congested the larger channels with excess cells in an effort to push past the clogs leading to the smallest channels. Tests run with younger cells did not produce these issues at all. In addition to taking a shorter time to seed, younger cells also seemed to cover more space within the smallest channels during seeding. Figure 23 below illustrates this effect.

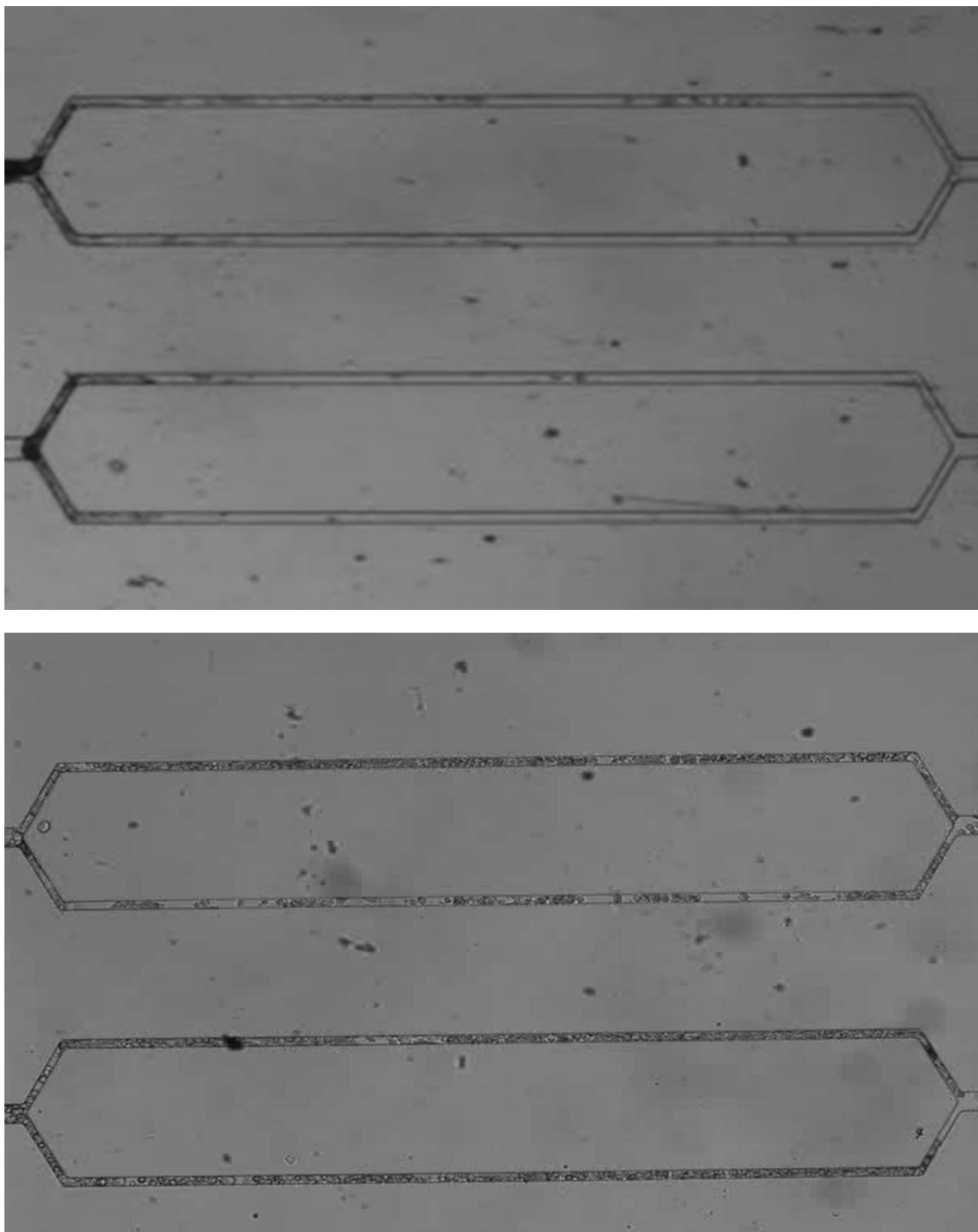


Figure 23: Seeding images of old cells (top) and young cells (bottom). The older cells (top, >40 population doublings) have a harder time entering the smallest channels and often form aggregations at junctions leading to the smallest channels. In order to shear these away, the inlet and outlet are reversed and flow rate is increased above 50 microliters/min. The younger cells (bottom, 16 population doublings) have an easier time entering the smallest channels and can even generate great coverage of the channels. They are also able to maintain their cell integrity and avoid cell death due to mechanical squeezing from seeding, which older cells have a more difficult time accomplishing.

3.6- Presence of Dextran, Percent Trypsin Used for Cell Preparation, and Incubation

Lifetime of Confluent Devices

Presence of Dextran in the Infusion Solution

We tested for the effect of Dextran 100 (ranging from 8-20% weight/volume) at both very low cell concentrations (1.5 million cells/mL) and at a concentration level that was known to generate successful seeding and growth (5 million cells/mL). This generates a range of viscosity increases by a factor of 10-80²⁵. This also covers the 20x viscosity increase generated by 8% Dextran 500 utilized in the Myers et al. protocol^{11,12}. We found that Dextran had no noticeably effect on the seeding process. Although Dextran caused the infusion solution moved through the channels at a slower velocity, the overall seeding and percent coverage of the smallest channels was virtually identical for tests with and without Dextran. The reason is that although Dextran slows down the velocity of the cells flowing into the device, it also increases the shear stress experienced by the cells (directly proportional to increases in viscosity) and subjects them to likely detachment.

Finally, it is worth noting that on a qualitative level, Dextran slowed the infusion process for 5 million cells/mL trial. The increased viscosity of the liquid tended to remove attached clusters quite easily, as it increases the shear stress experienced by the cells in a directly proportional manner (Equation 1 in Section 2.3). On a general scale, this meant that infusion had to occur at lower injection rates and more time had to be allowed for cells to attach every time that flow was stopped. It is hard to quantify the exact speeds and times for this process, and the exact procedure of the Variable infusion method is different every time it used. Despite this, we did note that for a 15% weight/volume mixture, the flow rate never exceeded 5-8 microliters/min and the entire process took roughly 2 hours when integrated with our “variable flow” method.

Percent Trypsin Used for Cell Preparation

The amount of trypsin used to detach cells from their culture flasks played a significant role in the seeding results. For our previously mentioned trials, we used both 0.025% and 0.05% trypsin. We noticed that 0.05% trypsin yielded better seeding results than 0.025% trypsin for seeding coverage within channels. Using 0.05% trypsin instead of 0.025% trypsin, percent coverage increased from 5% to 10% at 1.5 million cells/mL and from 20% to 30% at 4 million cells/mL. The reason behind this is likely because 0.05% trypsin made the cells less likely to aggregate in very large chunks and settle at the bottom of the injection syringe and/or to be too large to enter the device, which is in agreement with previous studies from our lab ²⁷.

In addition, we examined a wider range of elevated trypsin concentrations: 0.1% (75:25 ratio of 0.05% and 0.25% trypsin) and 0.15% (1:1 ratio of 0.05% and 0.25% trypsin) with a cell concentration of 5 million cells/mL. In both cases, the first 10-20 minutes of infusion consisted of mostly single cells entering and leaving the device without any substantial attachment. Eventually, clusters began to enter the device and we noticed junction clogging and some degree of attachment. However, we noticed that a significant amount of clusters contained cells in which the cell membranes were damaged. Furthermore, after incubation, many of these cells did not attach. Figure 24 below illustrates these observations. While these trypsin concentrations limited cluster formation, they damaged the ECs, preventing the cells from remaining viable.

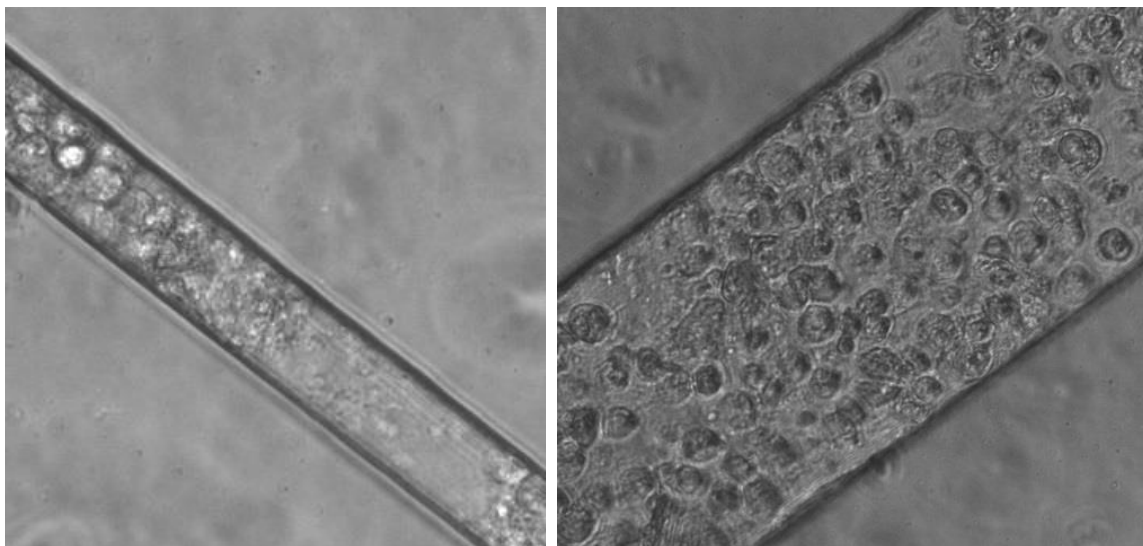


Figure 24: (Left)- Initial seeding within 20 micron channel (left) with 0.15% trypsin and 50 micron channel (right) with 0.1% trypsin (zoomed). (Left)- The cells no longer retain their circular shape and their membranes seem to be damaged. The contrast between damaged cells can be seen through the cell debris in the middle of the channel as opposed to live cells at either end of the channel. (Right)- 50 micron channel (zoomed in) two days after 0.1% Trypsin was used for cell preparation. No attachment can be seen as they still retain their circular shape, have not elongated, and remain in suspension. They were also observed to be sheared away at flow rates above 50 $\mu\text{L}/\text{min}$.

These findings are in agreement with previous work in our lab that shows endothelial cell detachment to be sensitive to trypsin concentration: higher concentrations prevent clusters from forming, but they also cleave integrins and reduce the likelihood of overall adhesion²⁷. We recommend using a final trypsin concentration of 0.05% for detaching cells from their culturing flasks. Preparing cell concentrations above 3.5 million cells/mL usually involves centrifuging detached cells that are suspended in a 10 mL solution of media/trypsin, aspirating out the liquid, and then re-suspending with media containing serum to match the desired concentration. Because of this process, it is also possible to add between 10-50 microliters of additional 0.05% trypsin to the media added to obtain the final cell concentration. This can act as a light anti-adhesive within the solution in case clogging becomes an excessive issue during seeding. In most cases, however, this will not be needed.

Incubation Lifetime of Confluent Devices

We found that, after 3-5 days of development within an incubator after seeding, the incubation

lifetime of already confluent endothelium while under continuous media flow between 0.5-3 $\mu\text{L}/\text{min}$ was generally 2-3 days. Afterwards, cells began to detach from the channels. In more extreme cases, the bonding between the PDMS and glass broke in the device and cells spilled out into previously bonded areas of the device, where they attached and potentially began to spread again. Figure 25 below illustrates a device beyond its incubation lifetime in 50 micron and 20 micron channels and illustrates the effect of cells peeling off channel walls.

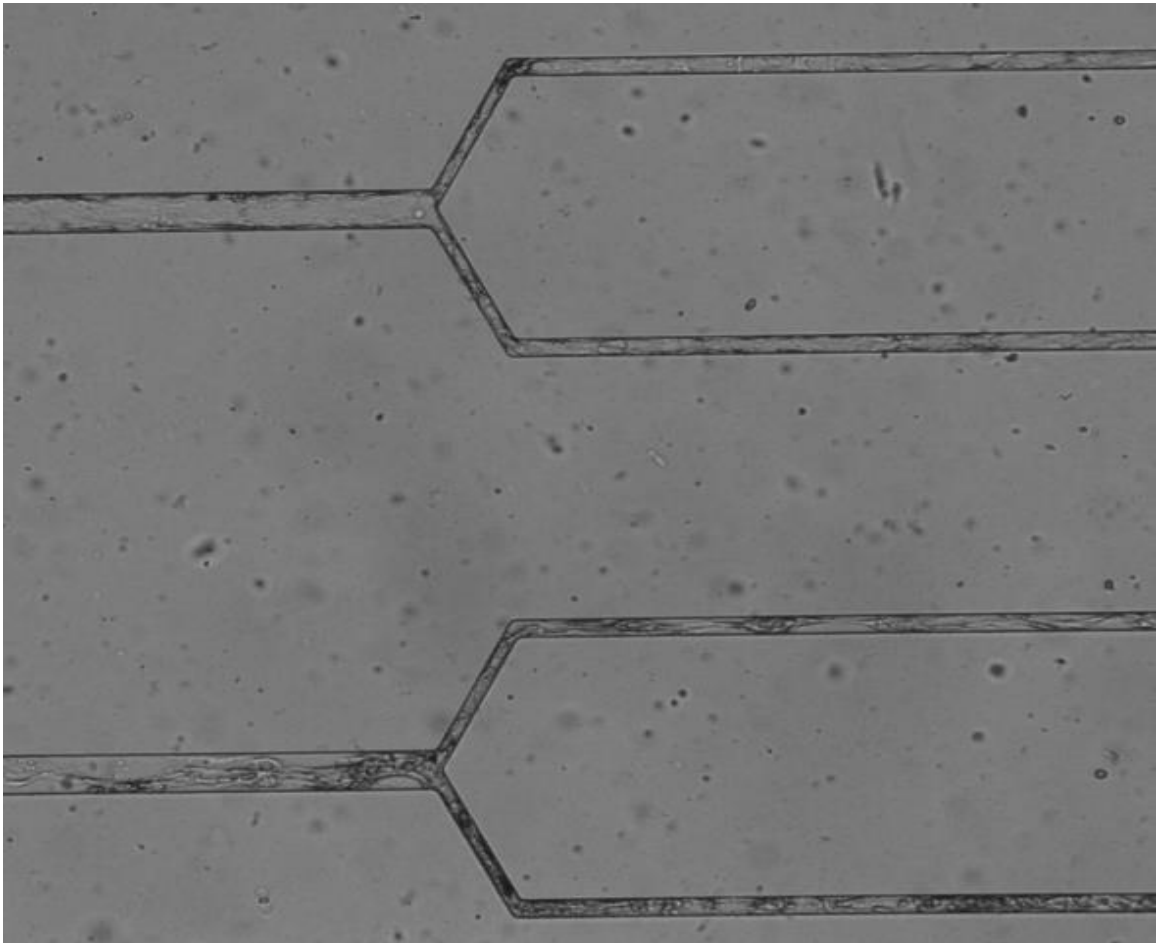


Figure 25: Brightfield image of 50 micron and 20 micron channels within a device 2 days after reaching confluency. The network on the top shows cells that have not yet begun to peel off due to aging. The network on the bottom shows cells that have already begun to peel off and shrivel. Cells seem to detach from the side walls and migrate toward the center of the channel when too old. The one exception is if the PDMS-glass bonding breaks due to internal pressure, upon which cells will spill outwards into previously bonded areas of the device.

3.7- Summary of Test Conditions

Table 5 below shows all of the conditions tested during infusion and their seeding results.

Table 5: Conditions used for infusion and their respective seeding results

* The base infusion volume used for each device was roughly 1 mL. Depending on the aggregations and Variable flow speeds used, this volume usually took around 1 hour to completely infuse into the device.

** Only channels that experienced at least 20% coverage became fully confluent after 4-5 days.

*** Larger channels experienced a high concentration of excess cell clusters. Some were excess clusters not attached to the channel walls and needed to be sheared or washed away after incubating. Flow rate used to wash these aggregations away was anywhere between 50 $\mu\text{L}/\text{min}$ to 100 $\mu\text{L}/\text{min}$ with base by flowing through base EBM-2 media.

**** Larger channels were too clogged with cells to allow proper cell attachment and growth of endothelium.

† Experiments done with Dextran were performed at very low flow rates (usually 0-5 $\mu\text{L}/\text{min}$)

<i>Cell Concentration (cells/mL)</i>	<i>% Trypsin</i>	<i>Dextran†</i>	<i>Flow</i>	<i>Seed Time, hours</i>	<i>% Coverage after Seeding Period</i>	<i>Successful Confluence after growth</i>
500,000	0.025%	Yes- 8%	Constant	2	< 1%	No
500,000	0.025%	No	Constant	2	< 1%	No
500,000	0.05%	Yes- 15%	Constant	2	< 1%	No
500,000	0.05%	No	Constant	2	< 1%	No
1,000,000	0.025%	Yes- 15%	Constant	2	< 5%	No
1,000,000	0.025%	No	Constant	2	< 5%	No
1,000,000	0.05%	Yes- 20%	Constant	2	< 5%	No
1,000,000	0.05%	No	Constant	2	< 5%	No
1,500,000	0.025%	Yes- 8%	Constant	2	< 5%	No
1,500,000	0.025%	No	Constant	2	< 5%	No
1,500,000	0.05%	Yes- 15%	Constant	2	< 10%	No
1,500,000	0.05%	No	Constant	2	< 10%	No
2,500,000	0.05%	Yes-15%	Variable	1*	<10%	No
3,000,000	0.05%	No	Variable	1*	<10-15%	No
3,500,000	0.05%	Yes-15%	Variable	1*	<20%	Yes**
3,500,000	0.05%	No	Variable	1*	<20%	Yes**
4,000,000	0.025%	No	Variable	1*	<20%	Yes**
4,000,000	0.05%	No	Variable	1*	<30%	Yes
5,000,000	0.05%	Yes-15%	Variable	2 *	<60%	Yes
5,000,000	0.05%	No	Variable	1*	<60%	Yes
5,000,000	0.10%	No	Variable	1*	<60%	No
5,000,000	0.15%	No	Variable	1*	<60%	No
5,500,000	0.05%	No	Variable	1*	<60%	Yes
6,000,000	0.05%	No	Variable	1*	<65%	Yes****
6,500,000	0.05%	No	Variable	1*	<65%	Yes****
7,000,000	0.05%	No	Variable	1 *	<80%	No****
8,000,000	0.05%	No	Variable	1*	Device Leak	N/A

3.8- Brightfield Imaging

After initial seeding, successfully seeded devices generally became confluent throughout all of their channels after 3-5 days of media flow (not including the 2-3 days lifetime after confluency) at 1.0 $\mu\text{L}/\text{min}$ and incubation at 37C. Figure 26 below shows that uniform confluence within the device channels. The example is a result of 5,000,000 cells/mL infusion concentration.

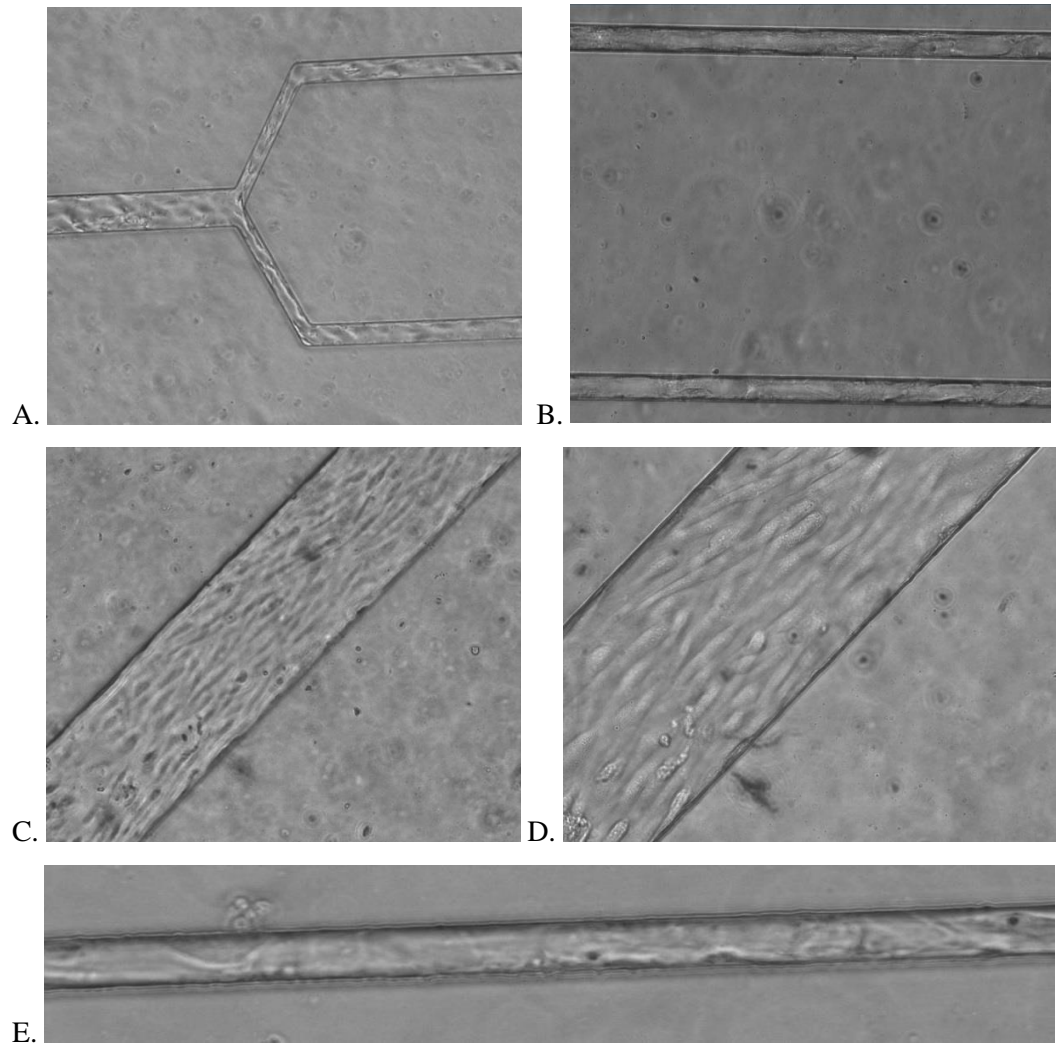


Figure 26: Brightfield images showing cell seeding within channels. (A) shows a 50 micron to 20 micron junction, (B) shows the middle of 20 micron channels, (C) shows the middle of a 200 micron channel, and (D) shows the middle of a 400 micron channel. (E) shows a zoomed view of a 20 micron channel. As channels grow larger, individual cells can be seen occupying greater volumes. This was the result of a 5,000,000 cells/mL concentration with 0.05% trypsin.

3.9- Immunofluorescent Imaging

Fully confluent devices were fixed and stained in accordance to the procedure outlined in the methods section. They were visualized for VE Cadherin interactions (green) and location of nuclei (blue). Figures 27 through 30 below show confluency for a 5,000,000 cells/mL infusion.

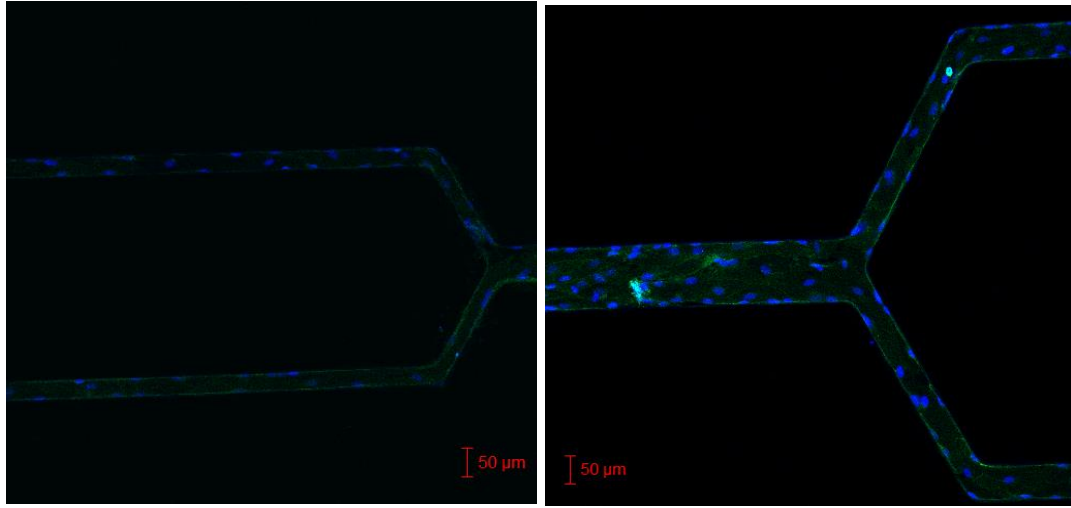


Figure 27: Confocal views of a 50 micron to 20 micron junction (left) and a 100 micron to 50 micron junction (right). Both pictures show DAPI nuclear staining (blue) and VE-Cadherin staining (green), demonstrating that the cells are uniformly spread but in contact with one another.

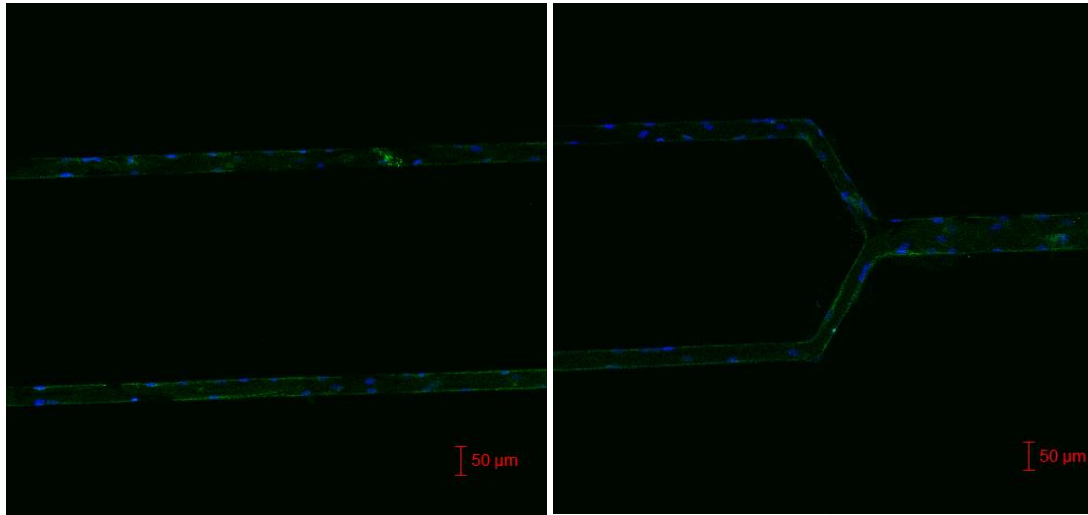


Figure 28: Confocal images of the middle of the 20 micron channels (left) and a 50 micron to 20 micron junction (right). Both images show DAPI nuclear staining (blue) and VE-Cadherin staining (green), demonstrating that the cells are uniformly spread and in contact with one another.

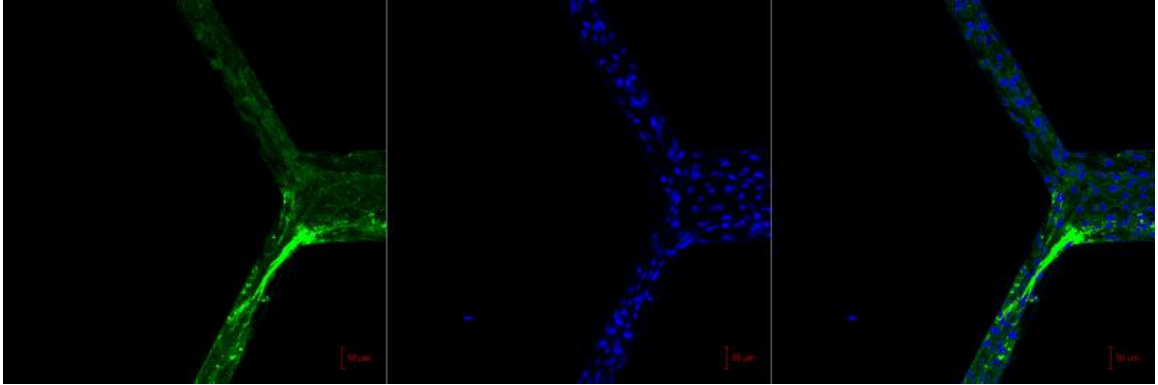


Figure 29: Confocal images showing cell seeding at a 200 micron to 100 micron junction. The picture on the left shows VE cadherin staining, the picture in the middle shows DAPI nuclear staining, and the picture on the right superimposes both VE cadherin and DAPI nuclear staining.

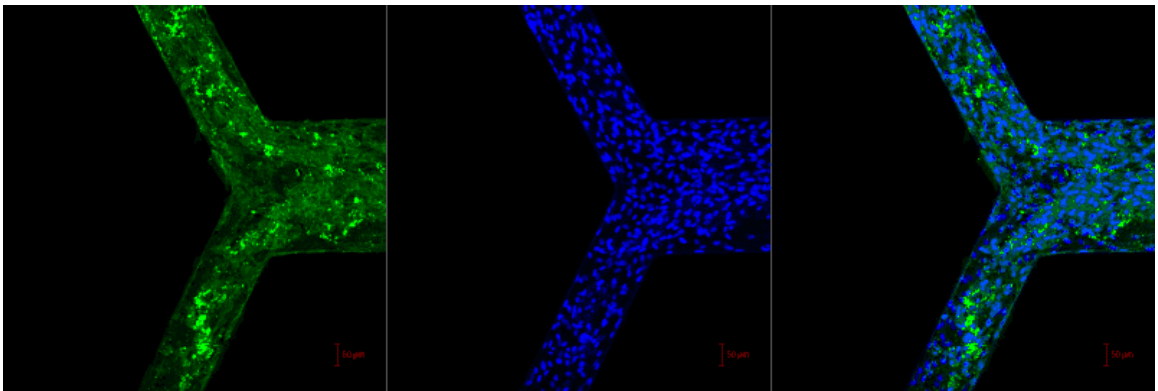


Figure 30: Confocal images showing cell seeding a 400 micron to 200 micron junction. The picture on the left shows VE cadherin staining, the picture in the middle shows DAPI nuclear staining, and the picture on the right superimposes both VE cadherin and DAPI nuclear staining.

3.10- Cell Coverage at Confluence

The density of cells within the 20, 50, 100, and 200 micron channels were estimated and plotted in Figure 31 below. For each channel, the total cell count within horizontal plane of view was taken and divided by the area that the channel occupied.

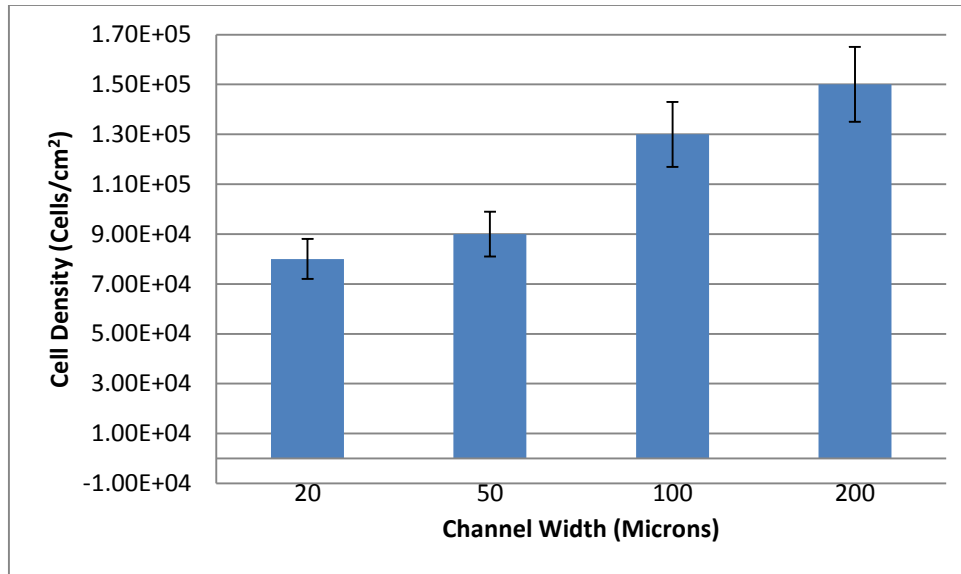


Figure 31: Confluent cell density within channels of a device (cells/cm²) seeded at 5,000,000 cells/mL.

These numbers are similar to other densities produced in our lab (80,000-150,000 cells/cm²). The reason why the 20 micron and 50 micron channels contain less cell density is perhaps due to endothelial cells being compressed more than usual while in an environment that is roughly microvascular in size. Another reason is perhaps due to the cells being in very tight contact with one another within these small channels, whereas within larger channels that are much more spacious they can spread and there sometimes may even be empty space between some cells. Ultimately, the trend of increasing cell density along with channel size shows that cells have to squeeze beyond their natural levels to fit within microvascular channels, which opens up the door for future studies on the effect of such squeezing on their physical and chemical behaviors *in vitro*.

3.11- Sickle Blood Flow Results

1 mL of fully recessive HBSS sickle blood was run through a confluent endothelialized device at physiological flow rates (0.7-1.0 µL/min to generate appropriate midstream velocities) and the

results were recorded on video. The flow lasted around 1 hour. Figure 32 below show results of the flow experiment in larger channels and helps to illustrate the stark contrast between “free space” (blood flow path) and the space taken up by endothelium (white space).

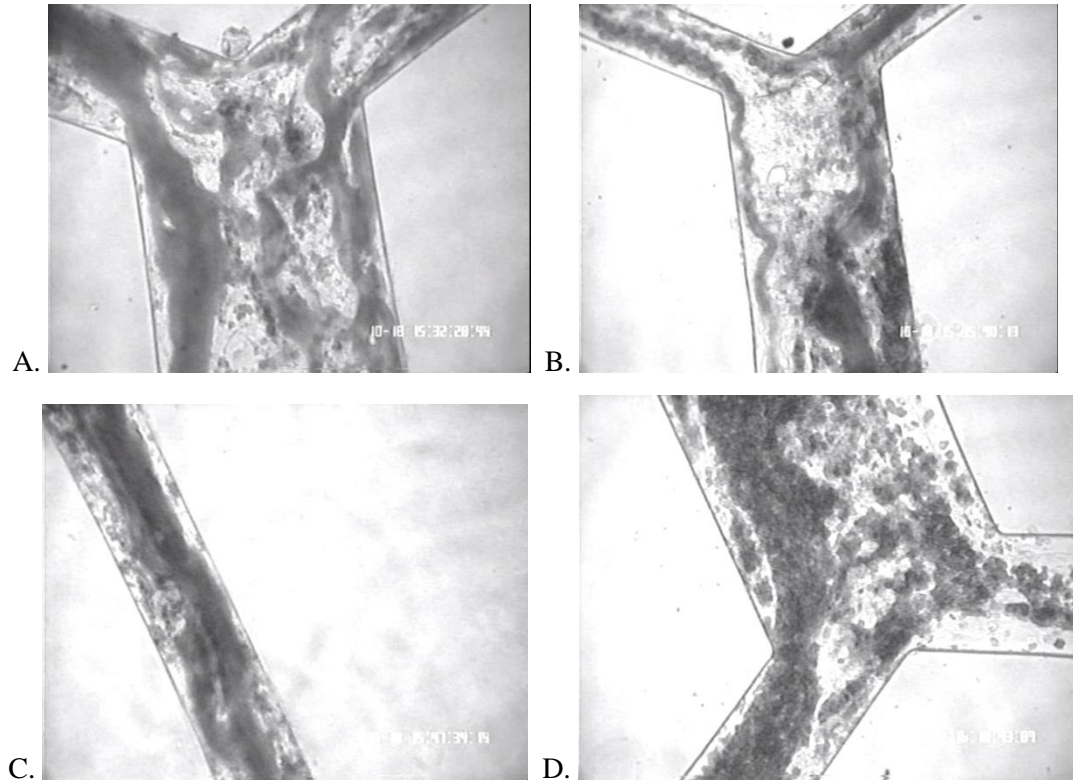


Figure 32: Screen captures of sickle blood flow experiment through endothelialized channels. (A) shows a 100 micron to 50 micron junction, (B) shows a 50 micron to 20 micron junction, (C) shows a 50 micron channel, and (D) shows another 100 micron to 50 micron junction. Note that the channel height is 30 microns in all cases. In cases where endothelium protrudes from both upper and lower borders to make boundary layer resistance high (randomly distributed throughout the channels), sickle blood will choose to avoid these pathways and flow in the paths of least resistance. A bolus is shown to be forming within (C) on the left-side of the channel wall, clearly impeding further flow in its space.

After the flow experiment, flow was halted to show the presence of endothelial aggregations within the channels. Figure 33 below shows sickle boluses adhering to endothelium after flow was stopped. The cells are dark in stark contrast to the endothelium, which appears grey and

white. Boluses are seen randomly scattered across the endothelium surfaces within each of the channels, which hints at scattered distribution of bolus formation.

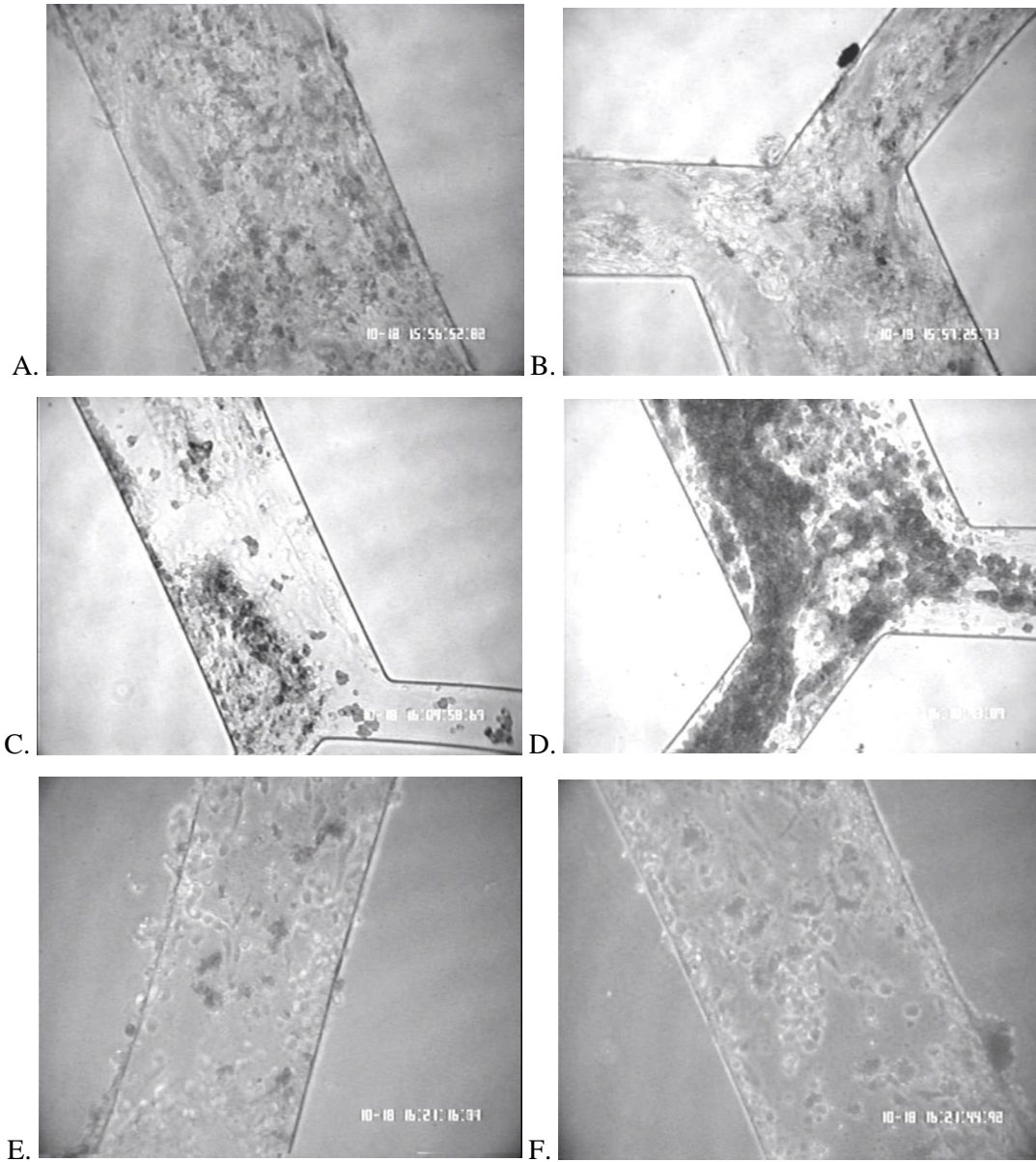


Figure 33: Endothelialized channels after sickle blood flow experiment. The flow rate in these images is at a virtual standstill. (A) shows sickle aggregations within a 100 micron channel, (B) shows aggregations within a 100 micron to 50 micron junction, (C) shows aggregations within a 50 micron to 20 micron junction, and (D) shows aggregations within another 100 micron to 50 micron junction. (E-F) show phase contrast images highlighting the presence of aggregations within 100 micron (E) and 200 micron (F) channels. Patches of dark spots (sickle cells) can be seen distributed across each of the channels, which is an indicator of bolus formation.

Within the 20 micron wide channels, sickle cells snaked around endothelial cells lining all sides of the device in almost a single-file fashion. This movement may be due to the protrusion of the nucleus. Only a small amount of cells could fit inside a channel at any given time. Figure 34 below highlights this phenomenon by showing both a standard brightfield image showing the general flow path and a phase contrast image that highlights the endothelium surrounding the cells.

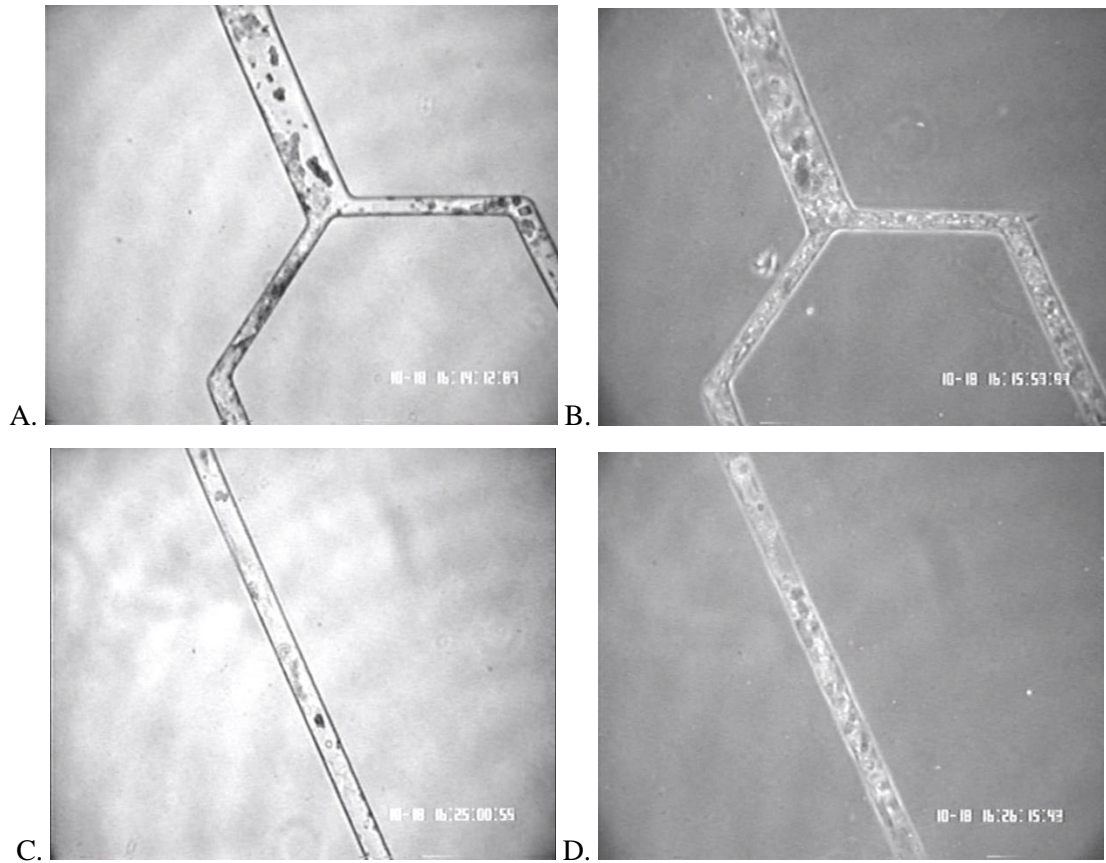


Figure 34: Sickle cell flow within a 50 micron to 20 micron junction (A,B) and the middle of a 20 micron channel (C, D). Panels on the left (A, C) show brightfield images in which sickle cells (very dark cells) flow through the channels in a single-file fashion; the white space lining the edges of the channels represents endothelium. The panels on the right (B, D) show phase contrast images in which the endothelium is clearly shown to occupy the white space from the pictures on the left.

Sickle cell aggregates sporadically formed within these small channels, although at a much lower frequency than in the larger channels. Figure 35 below shows two sickle cell aggregates within a 20 micron channel that was present both during flow and after the flow had been stopped.

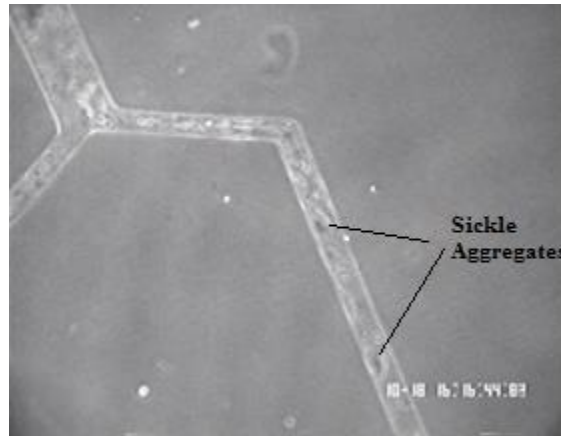


Figure 35: Phase contrast image showing sickle cell aggregations near a 50 micron to 20 micron junction. The aggregates can be seen as the two dark clusters within the 20 micron channel.

Based on these results, we can conclude that flows generating physiological midstream velocities within the smallest channels might cause a high likelihood for bolus formation within the larger channels. Since cells can only fit in one-at-a-time (or in small clusters) into the 20 micron channels, the likelihood of clogging is not too great. However, many clusters of cells are exposed to the vast amounts of endothelium leading up to these channels and have a far higher likelihood of adhering to their walls. Thus, sickle cell aggregate formation occurred randomly throughout the flow device.

We hypothesize that, as long as flow rate is not increased throughout the study, these aggregates will not be sheared away and will continue to grow if a greater volume of blood is run through the channels. Eventually, full vaso-occlusion may occur (similar to the clogging seen during the seeding process) in which the entire channel is covered with aggregated sickle cells.

However, the cell concentration of blood is much greater than that of the infusion solution. Thus, after clogging during the sickle flow experiment, there was not just “media” (or in this case, plasma) that ended up flowing through the channels- the cells could not be left behind inside the syringe. Within this experiment, cells were inevitably pushed into the device, which may have led to initial breakage of some of the clogs. More importantly, however, a leakage at the inlet of the device ultimately occurred due to high resistance buildup within the channels. This result is also in tandem with previous studies we performed with empty channels that also show that too much clogging leads to an eventual leads to an inlet leak, possibly ruining the device in the process. The inlet leak at the end of this experiment is shown in below in Figure 36.

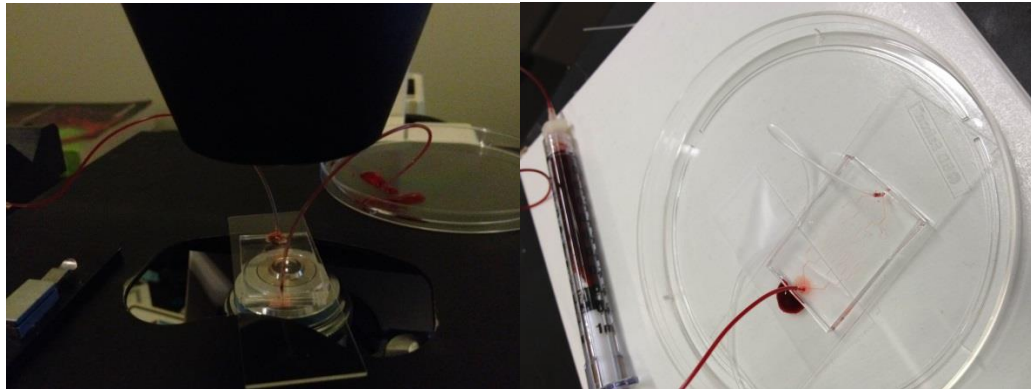


Figure 36: Leakage at the device inlet after buildup of resistance within channels during the sickle flow experiment. The picture on the left shows a leakage at the inlet region where the tubing connects to the device, which could not be prevented by wiping clear the leakage and reconnecting the tubing. In an effort to alleviate this, the inlet and outlet were switched and the flow was reversed. However, the picture on the right shows that the new inlet (previously the outlet) then leaked at the region where PDMS bonds to glass. This process is irreversible and destroys the device (the bonding of the inlet region to the glass slide is ruined), effectively rendering the experiment unable to continue.

The bursting of the inlet shown above is likely equivalent to what a diseased patient would experience during a vaso-occlusive crisis. Therefore, this platform can be used to simulate, from start to finish, the development of a crisis within a microvascular network. It can also be used to test anti-adhesive drugs that may or may not affect bolus formation during crises, such as propranolol²⁸ or metmorphin²⁹. Sickle blood that is coupled with such drugs can be flown

through these chambers and the effectiveness of these drugs can be evaluated by both the degree of bolus formation and whether or not resistive buildup ends up being too high in the device channels for further flow.

Chapter IV: Conclusion

This study ultimately outlines a novel, working, and reproducible seeding technique that allows a user to create a fully-seeded microfluidic device with long branching networks of channels of microvascular size (<30 microns). It takes into account the problems experienced by the previous studies and addresses them with the “Variable flow” technique outlined in the methods section.

We discovered that clogging is inevitable within long channel networks, and in order to overcome this obstacle, varying flow rates needed to be used in order to shear away aggregates at junctions. Correspondingly, the flow rate would needed to be lowered after aggregates were sheared way in order to allow for further cell attachment. Furthermore, a specific range of concentrations (3.5-7.5 million cells/mL) were found to work best and not generated insurmountable excess aggregates within channels. Finally, we performed both preliminary calculations and recorded cell seeding tests to make observations on cell seeding mechanics. Among our findings are notes on higher affinity of attachment for clusters of cells over individual cells, increasing cluster sizes needed to attach to wider channels, at least a 25% seeding coverage of smallest channels needed for cell growth, and increased deformability of young cells when entering the smallest channels.

Our method allows for the creation of a variable, functional, optically clear, and high-power *in vitro* microvascular test platform upon which studies on hematologic diseases can be performed. This is the first protocol that tackles both the seeding of long channels (on the order of cm) that are of microvascular width (<30 μm). In order to demonstrate the viability of this platform, we have run fully-recessive HBSS sickle cell blood into the device and observed interactions and aggregations of sickle cells to the endothelium inside the device. We found that sickle cells tend to aggregate in larger channels due to the channels providing more surface area for sickle clusters to attach to. Within the smaller channels, we found that only individual sickle cells or very small

clusters were able to enter and snake around endothelial protrusions with minimal aggregation.

4.1- Future Studies

Our seeding method can be improved through the implementation of microfluidic valves at the junctions of the device. This is particularly useful for selecting the channels that will receive flow during the process of shearing away aggregations and shutting off flow to channels that are not clogged. This will also ensure that elevated flow rates do not shear away any cells in unclogged channels that are currently in the midst of attachment. With a microfluidic valve system implemented, the seeding time could potentially be reduced to under 10 minutes for every device.

In addition, the implementation of pressure transducers underneath the channels in a PDMS bilayer or trilayer (to accommodate microfluidic valves) device would assist in automating the variable flow process. Channels that experience elevated levels of resistance could have increased flow rates selectively directed to them in order to shear away aggregates at junctions. A matlab program could be developed to regulate the process and integrate both a pressure-reading system and a valve system into an all-in-one seeding apparatus.

Finally, we made note of the increased deformability of younger cells as opposed to older cells in our Results section. During our trials, we noticed that younger cells were able to squeeze into the smallest channels with much more ease and without causing cells to lyse. More tests could be done on the deformability of individual endothelial cells in suspension to optimize the proper cell age for infusion into devices. It would be of particular interest to see on what parts of the cells that this extra deformability originates.

In order to further demonstrate the power of this device, additional studies should be performed in which the flow experiments can be imaged at higher resolutions and in different styles. This will allow us to obtain truly novel results that cannot yet be obtained from other *in vivo* or *in vitro* studies. A novel technique known as wide-field digital interferometry (WFDI) can be used to measure the biomechanical properties of sickle cells and their aggregates on endothelium³⁰. This technique allows real-time scale surface fluctuations with a sensitivity scale of microns. In addition, it can help to visualize the biomechanical properties of sickle aggregations under various flow conditions and while being subject to factors such as treatment drugs. Even without WFDI imaging, the effectiveness of drugs can still be tested on this platform. Sickle blood that is coupled with anti-adhesive drugs can be run through the device and the flow properties within the channels can be monitored. Resistive buildup is an excellent measurement tool, and if a “crisis” (leakage at the inlet) can be avoided, successful studies of this nature can have a good reflection on the general effectiveness of certain drugs.

Appendix A: Protocol for Microfluidic Device Fabrication

Truskey Lab

PDMS Microfluidic Channel Creation Protocol

This is a protocol for creating a PDMS microfluidic channel from a silicon wafer template. It is split into the following sections:

Section A: Silanization of the silicon wafer and petri dish

1. Take two empty and sterile petri dishes and place them in the fume hood. On the first one, place the clean etched silicon wafer. On the second dish, place **4-5 drops** of tridecafluoro-1,1,2,2-tetrahydrooctyl)-1-trichlorosilane. This chemical is toxic and corrosive, so it is important to conduct all steps in the section in the hood.
2. While leaving both dishes uncovered, place them into the vacuum dessicator and turn on the vacuum. After 15 seconds, turn the knob on the dessicator to disconnect airflow, disconnect the vacuum tube from the dessicator, and turn off the suction from the fume hood. The apparatus will remain under vacuum as no air will be allowed to flow inside.

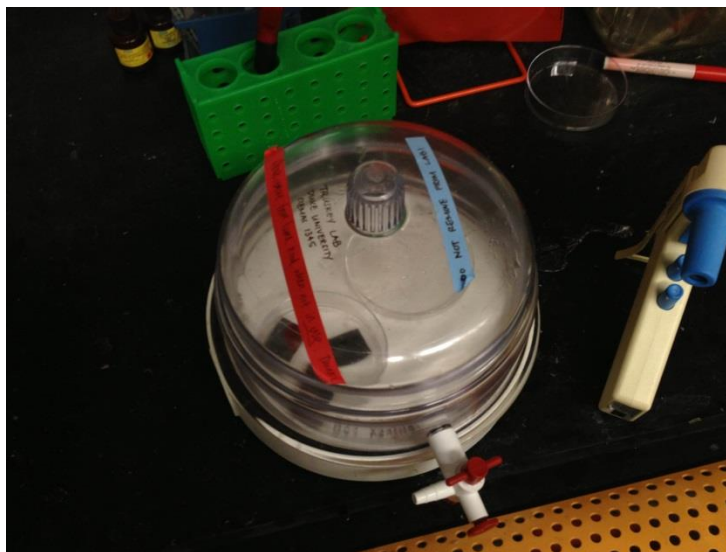


Figure 1: 2 dishes in vacuum. One dish has a few drops of silanizing agent, the other has 3 silicon wafers

Leave the apparatus under vacuum for around 10 minutes. This allows the tridecafluoro-1,1,2,2-tetrahydrooctyl)-1-trichlorosilane to deposit in a uniform layer onto the metallic template. The purpose of this step is to generate a hydrophobic layer on the plate and petri dish that allows for easy PDMS removal.

3. Remove both dishes. Place the dish that originally had a few drops of tridecafluoro-1,1,2,2-tetrahydrooctyl)-1-trichlorosilane into a red hazardous waste bag and discard

appropriately. Cover the silicon wafer petri dish until ready for further use in the next section.

Note: every time you re-use a wafer, you do not have to re-silanize it. You should still silanize a new petri dish every time you make molds though.

Common mistakes- Avoid the following:

- a. Placing too many drops of tridecafloro-1,1,2,2-tetradydrooctyl)-1-trichlorosilane onto the second empty petri dish during step 1. Doing so will cause the entire vacuum dessicator to fog up during vacuum and too much chemical to be deposited onto the other petri dish and metallic template. Consequences of this include excessive bubbling reactions upon PDMS placement into the first petri dish-template apparatus and a sticky, non-clear, and gelatinous microfluidic channel as an end product.*
- b. Placing the tridecafloro-1,1,2,2-tetradydrooctyl)-1-trichlorosilane onto the same plate as the silicon wafer during step 1. This will cause the etched surface of the silicon wafer to be covered with a thick and “goopy” layer, potentially ruining the etchings on its surface.*
- c. Letting the tridecafloro-1,1,2,2-tetradydrooctyl)-1-trichlorosilane directly touch the surface of the silicon wafer. This WILL ruin the template and should be avoided at all costs.*
- d. Letting the apparatus sit under vacuum for too long. This will cause excess and sticky silane residues to deposit unevenly onto the wafer, making the surface sticky and unsuitable for molding.*

Section B: PDMS Deposit

1. Weigh out approximately 30 grams of PDMS using a weighing boat and a tared weighing system.
2. Using a micropipetter, extract 3 ml of PDMS curing solution (a 10:1 ratio of PDMS to curing solution) and pipette the contents into the weighing boat that contains the PDMS. It is best to pipette the contents out while the tip is slightly above the surface of the PDMS in order to minimize bubbling.
3. *Stir the mixture very gently for ~1- seconds with the same pipette that was just used in order to evenly distribute the curing agent into the PDMS.*

4. Uncover the petri dish with the metallic template from Section A and pour the PDMS into the dish.
5. Place the dish into the vacuum dessicator and proceed to vacuum for 60 to 90 minutes. This process is performed in order to remove air bubbles within the PDMS mixture.
6. Remove the dish from the dessicator. *Chances are that there may still be bubbles or residues left on or inside the PDMS surface.*

VERY IMPORTANT: Scalpel blade post-processing

If there are bubbles or residues still left on/inside the PDMS, use a thin edge (a scalpel blade works well) to gently push the bubbles to the side and or pop the bubbles. The bubbles can be popped by gently putting the blade next to the bubble and then lifting up and setting the blade down back onto the PDMS (do not let the entire blade leave the PDMS surface, otherwise this will create new bubbles).

If there are any particles that get onto the surface, you can also use a blade to push them aside.

Finally, there may be dust that somehow got trapped in the middle layers of PDMS (not fully vacuumed to the surface). You can also use a blade to push this to the side and scoop it out.

In the end: Be sure that the entire PDMS layer that immediately covers the silicon wafer is completely clear and free of all bubbles and particles.

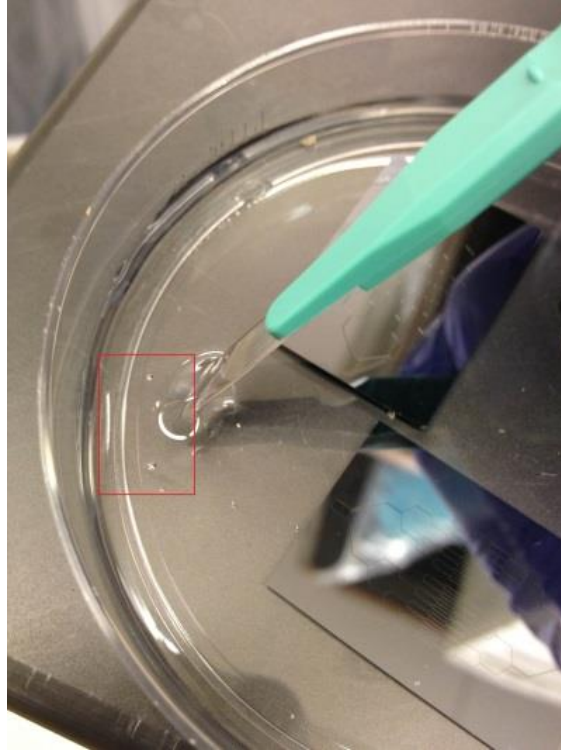


Figure 2: Using razor blade to push aside bubbles and particles. The red box indicates areas with bubbles.
Common Mistakes-Avoid the following:

- a. Placing a highly excessive amount of curing agent into the PDMS in step 2. This will cause excessive bubbling that is impossible to get out within a reasonable vacuum period.*
- b. Stirring the mixture vigorously or excessively in step 3. This will also cause excessive bubbling in the PDMS mixture.*
- c. Aggravating or touching the surface of the metallic template during removal of residual bubbles in step 6. This will ruin the template surface and damage your resulting microfluidic channel.*

7. After clearing the surface of residues, turn on the oven in the lab to the “2” power setting on the knob. This corresponds to approximately 60 degrees Celsius. Allow it to preheat for 15 minutes.

Place the PDMS mold and petri dish (UNCOVERED) into the oven and bake for 2 hours. If the PDMS is not sufficiently hard after this time period, keep baking the mold in 15 minute intervals and monitor its progress. Once the hardness is sufficient, remove the mold from the oven and allow it to cool for 5 minutes.

(Note: You can also just let the mold sit for 48 hours at room temperature to cure. If you choose to do this, leave the petri dish covered so that particles do not get onto the PDMS surface)

Section C: PDMS Removal and Shaping the Channel

1. After baking the mold, let it cool down for 5 minutes and then begin working on it. If you wait too long, it will grow cold and will become harder to remove.

If you allowed the mold to cure at room temperature, try to heat it up a little (place it in a 60 degree oven for 3-5 minutes) to make removal a bit easier.

2. Take a scalpel or sharp flat edge and dig straight into the PDMS next to the edge of the petri dish. After digging into the PDMS, you can use this leverage to pry the entire PDMS mold out of the petri dish.
3. After prying the PDMS out, the wafers should have a thin layer of PDMS that got underneath during the molding process. This will get in the way of removal and must be removed. Use a razor blade to slowly cut away edges as you peel back the PDMS to make for easy cutting.



Figure 3: Cutting away PDMS edges

4. After you have cut away 3 of the edges, slowly peel the PDMS off of the excess PDMS cover layer.

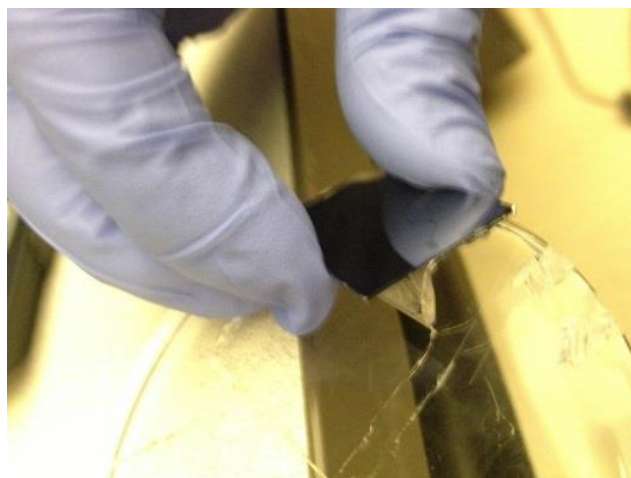


Figure 4: Peeling away PDMS from excess cover layer

5. Use a razor blade to slice into the PDMS such that template-etched portion of the PDMS is cut out.

-IMPORTANT: It is crucial to not make continuous “bread-knife” cuts that involve the blade going up and down. This can potentially cause the PDMS to crack and the shape of the resulting channel to be uneven. Instead, simply press down *firmly* with the razor blade and slice through in one slow motion for each direction that you are cutting.

6. Dispose of the non-templated PDMS in a red hazardous waste bag.
7. ***Be sure to punch entry and exit holes for flow*** into the PDMS before you begin section D.
 -Be sure to start punching on the side that has the pattern engraved onto it. This way, you can be sure that you won't miss the inlet or outlet while punching the hole.
 The pink-colored hole puncher in our lab works best. The diameter of this hole puncher is 1.66 mm.
8. The newly etched and shaped PDMS mold should be stored in a safe and dry location until it is bonded to glass in section D.

Common Mistakes- Avoid the following

- a. Excessively bending the PDMS. The cured PDMS is relatively hard and does not have much flexibility. Bending it can cause chunks to break off.

- b. Cutting too close to the etched area. Since the cutting motion may not be 100% accurate, cutting too close may result in etched portions being removed from the resulting microfluidic channel. It is best to cut at the boundaries of the templated area, as they already have more than enough separation from the etched areas.
- c. Punching the inlet/outlet holes by starting on the non-etched side- It is hard to make sure that your hole puncher will exit exactly where your inlet and outlet need to be on the patterned side

Section D: Bonding the slides using ASHE1 in the SMIF Facility

1. Obtain training in order to use the plasma asher (ASHE1) in the SMIF facility's clean room

2. Prepare the Glass Slide(s)

1. (Optional)- Autoclave the glass slides.
2. (Important)- Clean the glass slides using a waterbath sonicator. The procedure is as follows:
 - a. Create a 2% PCC 54 detergent solution. This consists of 200mL deionized water and 4ml of PCC.
 - b. Pour deionized water into the waterbath sonicator until it reaches the notch on the side.
 - c. Place glass slides in a glass slide rack. Pour the 2% PCC solution into the slide rack until it fills up past the top of the slides.
 - d. Place the slide rack into the sonicator and sonicate for 10 minutes.
 - e. Remove the slide rack and pour out the remaining detergent solution. Rinse the slides by filling and removing the slide rack with tap water three times.
 - f. Repeat the rinsing two more times, except now with deionized water.
 - g. Take 5mL of MeOH and 5mL of HCl and mix them together into a clean beaker. Dilute the solution with deionized water until the volume reaches 200mL.
 - h. Pour the 1:1 MeOH:HCl solution into the slide rack until the slides are completely immersed and place it into the sonicator. Sonicate for 10 minutes.
 - i. After sonication, let the rack sit still in the sonicator for 10 minutes and then activate the machine to sonicate for another 10 minutes.
 - j Remove the slide rack from the sonicator and pour out the MeOH:HCl solution.
 - k. Like before, rinse the slides three times with tap water and two times with deionized

water.

- l. Pour in deionized water until the slides are completely immersed and sonicate these slides for 2 minutes.
 - m. Remove the slide rack, pour out the deionized water, and rinse once more with deionized water.
 - n. Remove all liquids from the slide rack and immerse these slides in 70% ethanol.
 - o. After 10 minutes, pour out the 70% ethanol and allow these slides to dry in the fume hood overnight. They are now clean!
3. After the glass slides are clean and have been dried, place them in a clean petri dish. Take thawed (liquid) PLL solution and add just enough solution such that the top of each slide is fully covered with liquid. This should amount to approximately 2-3 mL of solution per slide.
 4. Cover the petri dish and let the PLL solution sit on top of the glass slides for 3 days (this amount may be able to be reduced, although it has not been tested yet).
 5. Afterwards, remove any remaining PLL solution from the dish. ***Be sure to keep track of which surface of the slide is the activated one.*** Rinse the slides with deionized water three times.
 6. After rinsing, immerse the slides in deionized water for a minimum of three hours. Then remove the water and place the slides on a slide rack and allow them to dry overnight. These slides are now ready to be bonded to PDMS!

Preparing the PDMS for bonding

1. Take the PDMS you made in section C and apply scotch tape on both sides. Press firmly on either side and remove the tape. This removes residues that are sticking onto the PDMS.
2. (Optional) Take the PDMS and soak it in 70% ethanol. After 10 minutes, pour out the ethanol and examine the PDMS.
-This process may leave residues onto the PDMS and should be used with care.
3. If there are still residues remaining, let the PDMS dry in the fume hood for 5-10 minutes and then repeat steps 1 and/or 2 until the PDMS is completely clear and clean.
4. Let the PDMS sit in the fume hood until the glass slides are ready to be attached to the PDMS.

Using ASHE1 at the SMIF Facility to bond PDMS to glass

1. Take as many petri dishes as bonded molds you plan on making

-In each dish, place one PDMS mold and one glass slide
2. Bring scotch tape with you to the SMIF facility (This is VERY IMPORTANT)
3. When you get into the clean room, find the ASHE1 machine.

Open the tray and place two-three long pieces of scotch tape onto the tray (side-by-side with each other). This will act as a protective layer to place your PDMS onto. (If you do not do this step, there is a chance the PDMS will bond to the metal tray during ashing). Close the tray without placing anything else into the machine.

Use the following settings:

Power 100, Exposure time: 6 minutes, everything else default

Turn the machine on at these settings. This step will help the machine clean itself and the pieces of scotch tape you placed inside.

4. While the machine is running, thoroughly clean your PDMS mold again to remove any dust or residues that may be on there. This can be accomplished by using scotch tape and taping/removing it from the PDMS surface.
5. When the machine is done cleaning, let it cool down and then open the tray. Place the PDMS, *with the patterned side facing UP*, onto the scotch tape platform you created onto the tray. Next, place a glass slide next to (but not touching) the PDMS mold.
6. Close the tray and input the following settings into the machine:
Power: 19 watts, exposure time: 39 seconds, everything else default

Note: The power may vary depending on the hardness of your PDMS. If your PDMS is very hard, you can increase the power to 21-23 watts. If your PDMS is relatively soft and almost sticky, lower the power to 17-19 watts.

Turn on the machine to allow the ashing process to begin.

Important: be ready to begin the next step as soon as the ashing is done. Waiting or wasting time will cause this step to be completely ruined and you will have to start the ashing process over again.

7. As soon as the machine is done ashing and cooling, open the tray and immediately set the PDMS, *with the patterned side facing DOWN*, onto the glass.

Be sure to set the PDMS onto the surface of glass that was facing up while ashing.

Important: do not press too hard while setting the PDMS onto the glass. Only press very gently. If you press too hard, you run the risk of having the roofs of the channels bond to the glass as well, which will cause the channels to permanently collapse and ruin your entire mold.

If you made your PDMS properly, cleaned the PDMS and glass thoroughly, and used the settings listed above, your mold should end up fully bonded and ready to go!

8. **Important: Re-bonding incompletely bonded molds:** There is a chance that your mold may not be fully bonded after the last step (see figure below)

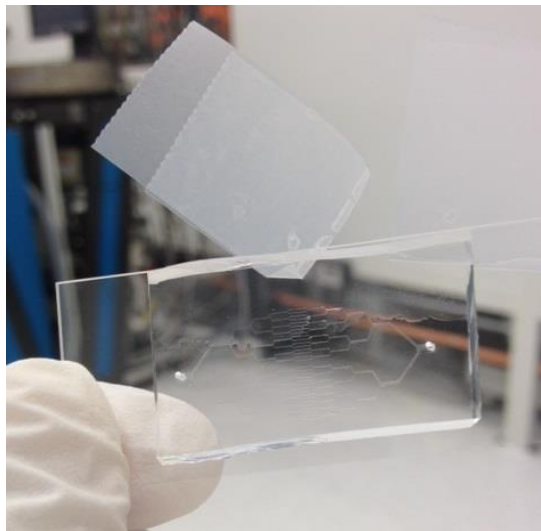


Figure 5: Partially bonded mold

If this is the case, open the ASHE1 tray place the mold onto the tray again (glass side facing down). Place a folded piece of scotch tape in between the mold and the glass. Close the tray and use the following settings:

Power: 65, Exposure: 25 seconds, everything else default

Run the ashing process at these settings. As soon as it is done, open the tray and press down gently on the un-bonded areas and this will cause them to bond onto the glass.

You may have to repeat this step several times to get all of the un-bonded regions to fully bond. Sometimes they will never bond no matter how hard you try and/or the mold just turns out to be un-usable. A lot of this will depend on luck and your technique with pressing down onto the mold.

You may alter the power and exposure time on this re-bonding step if you feel like it will make your molds bond better.

Common mistakes to avoid:

There is literally so much that can potentially go wrong with this that nothing is “uncommon.” I have yet to fully get my success rate above ~80%.

Appendix B: Protocol for Blood Flow into Microchannels

Truskey Lab

PDMS Microfluidic Channel Blood Flow Protocol

This is a protocol for creating a PDMS microfluidic channel from a silicon wafer template. It is split into the following sections:

Section A: Tubing Preparation

1. Take female 1.6mm inner diameter leuc locks and glue them onto the ends of PE 90 tubing.
-Be sure to glue the leuc locks so that the lock is facing outside. See figure 1 below for more details.

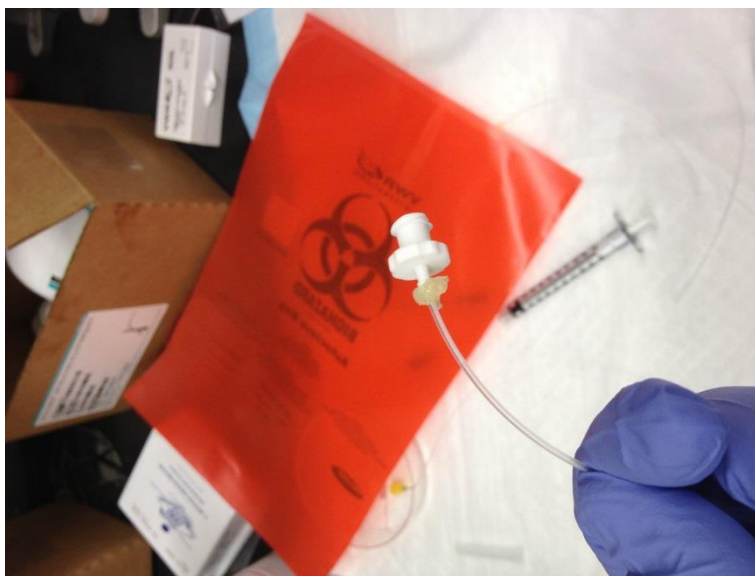


Figure 1: Leuc lock glued to the end of tubing

2. Take a syringe and place a magnetic stir bar or metal screw inside. This will help with stirring the blood later on while it is inside the syringe. Typically, the syringe will be a 3CC (3mL) syringe.

Section B: Microscope Room Preparation

1. Go into the back room and turn off all the lights.
2. Turn on the microscope. Place your microfluidic device onto the microscope and focus the image so that you can see all of the channels

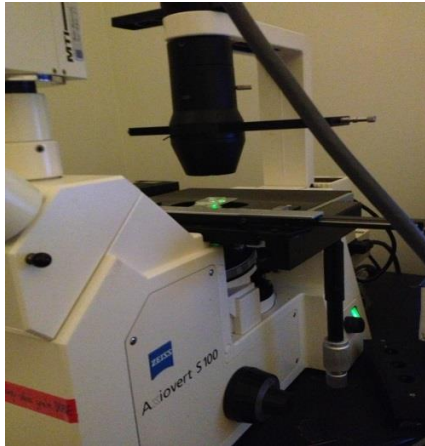


Figure 2: Microfluidic device focused on microscope

3. Turn on each of the machines by the TV. They are already calibrated, so you shouldn't have to touch anything else.
4. Be sure to set the time stamp to the correct date and time. It is the upper-most machine on the stack of machines. Press start on the machine when you are done so that time can start running.
5. Place an empty VHS into the VHS recorder



Figure 3: Image translated onto TV with timestamp running

6. Bring the Harvard PHD 2000 flow machine into the back room, plug it in, and turn it on. Set the refill rate to maximum (10 ml/min) and allow the machine to refill so that you can fit the entire length of the syringe tail onto the machine.

Important: be sure to set the diameter of the machine every time you use it. Different syringes have different diameters. For a 3cc (3mL) syringe, use a diameter of 10mm.

Important: Be sure to perform section C and D in quick fashion. This will prevent blood from settling or clogging inside the device or tubing. If it does clog, it is hard to get it unclogged and not have leakage from the device.

Section C: Blood Preparation

1. Obtain vials of blood from the Duke hospital.
2. Let the blood sit in a refrigerator, while standing vertically upwards, for 2-3 hours. This will cause the blood to separate via gravity into layers of plasma (upper layer) and red cells (lower layer).
3. After gravity separation, take the blood vials and place them into a biological hood. Also, take Dulbecco's Phosphate Buffered Saline (DPBS) and place it into the biological hood as well. Take a petri dish, a syringe, and leur lock/tubing set into the hood as well. Be sure to sterilize each item with ethanol spray before you place them into the hood.
4. Mark the top level of plasma on the vial with a marker. Uncap the vial and then aspirate out the plasma so that only red cells are left.

5. Add in DPBS to the exact same level as marked onto the vial. This helps keep the hematocrit at the same level as it was before.
6. Cap the vial and shake it up briefly to mix the contents.
7. Uncap the vial and pour it into a petri dish.
8. Take the petri dish and tilt it slightly sideways so that all of the blood concentrates towards one edge. This will help avoid extracting air bubbles when you use a syringe to extract the blood.
9. Take a syringe and place it at the edge where blood is heavily concentrated. Extract out as much blood as possible without getting air bubbles into the syringe.
-Take your leuc lock (with tubing glued on) and screw it onto the end of the syringe. This will effectively attach tubing your syringe
Important: Try to have as little blood as possible enter the tubing. This will prevent blood from clogging the tubing prematurely.
10. Dispose of the empty vial and bloody petri dish in a red hazardous waste bag.
11. Spray down the biological hood and follow standard cleaning procedures to ensure that the hood is disinfected after you are finished

Section D: Flow

1. Take the leuc-locked syringe (with blood) and a petri dish into the back room.
2. Take a ready-made PDMS microfluidic device and place an empty piece of tubing into the outlet.
3. Shake the syringe slightly to prevent blood from settling inside the syringe. Next, place the syringe onto the Harvard PHD 2000 flow machine.
4. Calibrate the flow machine so that the syringe fits snugly inside and that the tail of the syringe is being pushed against by the machine's flow diaphragm. This will make the syringe ready to for flow.
5. Take the end of the tubing from the syringe and place it snugly into the inlet of your microfluidic device. Place the device on the microscope stand.
6. Take the exit tubing from the outlet of the PDMS device and feed it into the empty petri dish. This will act as a disposal unit for flowed blood.
7. Press record on the VHS machine (it should already have an empty VHS cassette inside from section B).
8. Set the infuse rate on the Harvard apparatus to .07 ml/min and begin infusing blood.
9. Sit back and watch the magic happen!

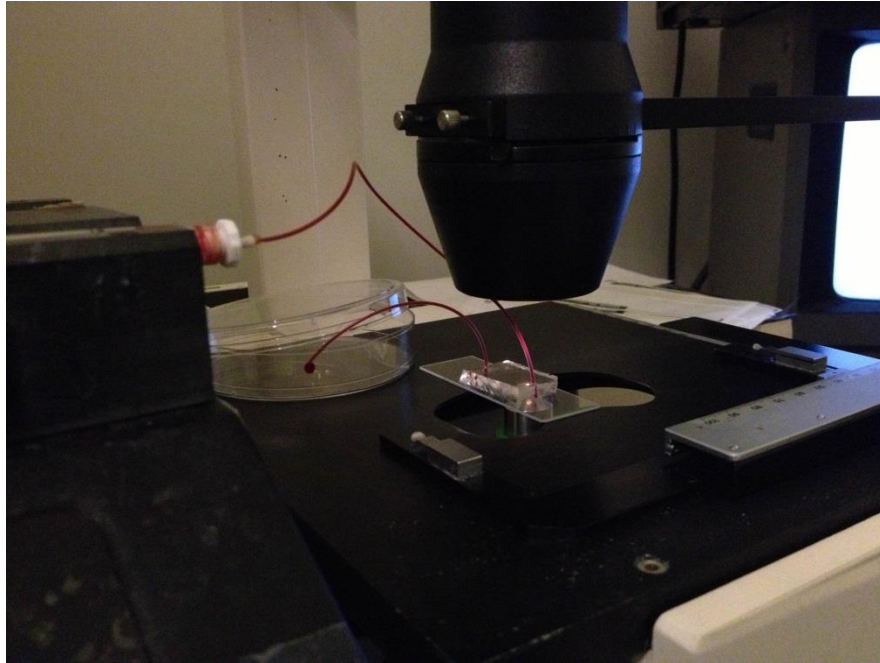


Figure 4: Flow experiment being conducted and recorded on a microfluidic device

10. After the flow is done, rewind the tape and press play to view the flow you just captured. In order to take computer screenshots of the flow, follow the instructions taped onto the side wall. They will instruct you how to use ImageJ and the “Scion” plugin to capture images of the video

References

1. Bunn, H.F. Pathogenesis and treatment of sickle cell disease. *N Engl J Med* **337**, 762-769 (1997).
2. Franchini, M., Gandini, G., Di Paolantonio, T. & Mariani, G. Acquired hemophilia A: a concise review. *Am J Hematol* **80**, 55-63 (2005).
3. Lawrence, J.B. et al. Hematologic manifestations of systemic mast cell disease: a prospective study of laboratory and morphologic features and their relation to prognosis. *Am J Med* **91**, 612-624 (1991).
4. Bourges-Abella, N.H., Reynolds, B.S., Geffre, A., Braun, J.P. & Trumel, C. Validation of the Medonic CA620/530 Vet 20-microl microcapillary sampler system for hematology testing of feline blood. *J Vet Diagn Invest* **21**, 364-368 (2009).
5. Groner, W. et al. Orthogonal polarization spectral imaging: a new method for study of the microcirculation. *Nat Med* **5**, 1209-1212 (1999).
6. Whitesides, G.M. The origins and the future of microfluidics. *Nature* **442**, 368-373 (2006).
7. Lee, C.Y., Chang, C.L., Wang, Y.N. & Fu, L.M. Microfluidic mixing: a review. *Int J Mol Sci* **12**, 3263-3287 (2011).
8. Mark, D., Haeberle, S., Roth, G., von Stetten, F. & Zengerle, R. Microfluidic lab-on-a-chip platforms: requirements, characteristics and applications. *Chem Soc Rev* **39**, 1153-1182 (2010).
9. Marre, S. & Jensen, K.F. Synthesis of micro and nanostructures in microfluidic systems. *Chem Soc Rev* **39**, 1183-1202 (2010).
10. Zhang, P., Murthy, Radisic A standalone perfusion platform for drug testing and target validation in micro-vessel networks. *Biomicrofluidics* **7**, 13 (2013).
11. Myers, D.R. et al. Endothelialized microfluidics for studying microvascular interactions in hematologic diseases. Jun 22;(64). pii:3958. doi: 10.3791/395 *J Vis Exp* (2012).
12. Tsai, M. et al. In vitro modeling of the microvascular occlusion and thrombosis that occur in hematologic diseases using microfluidic technology. *J Clin Invest* **122**, 408-418 (2012).
13. Esch, M.B., Post, D.J., Shuler, M.L. & Stokol, T. Characterization of in vitro endothelial linings grown within microfluidic channels. *Tissue Eng Part A* **17**, 2965-2971 (2011).

14. Rosano, J.M. et al. A physiologically realistic in vitro model of microvascular networks. *Biomedical microdevices* **11**, 1051-1057 (2009).
15. Ingram, V.M. A specific chemical difference between the globins of normal human and sickle-cell anaemia haemoglobin. *Nature* **178**, 792-794 (1956).
16. Kaul, D.K., Fabry, M.E. & Nagel, R.L. Microvascular sites and characteristics of sickle cell adhesion to vascular endothelium in shear flow conditions: pathophysiological implications. *Proc Natl Acad Sci U S A* **86**, 3356-3360 (1989).
17. Kaul, D.K., Chen, D. & Zhan, J. Adhesion of sickle cells to vascular endothelium is critically dependent on changes in density and shape of the cells. *Blood* **83**, 3006-3017 (1994).
18. Okpala, I. Leukocyte adhesion and the pathophysiology of sickle cell disease. *Curr Opin Hematol* **13**, 40-44 (2006).
19. Setty, B.N., Kulkarni, S. & Stuart, M.J. Role of erythrocyte phosphatidylserine in sickle red cell-endothelial adhesion. *Blood* **99**, 1564-1571 (2002).
20. Haynes, J., Jr., Obiako, B., King, J.A., Hester, R.B. & Ofori-Acquah, S. Activated neutrophil-mediated sickle red blood cell adhesion to lung vascular endothelium: role of phosphatidylserine-exposed sickle red blood cells. *Am J Physiol Heart Circ Physiol* **291**, H1679-1685 (2006).
21. Mohandas, N. & Evans, E. Adherence of sickle erythrocytes to vascular endothelial cells: requirement for both cell membrane changes and plasma factors. *Blood* **64**, 282-287 (1984).
22. Cheung, T.M., Ganatra, M.P., Peters, E.B. & Truskey, G.A. Effect of cellular senescence on the albumin permeability of blood-derived endothelial cells. *Am J Physiol Heart Circ Physiol* **303**, H1374-1383 (2012).
23. Brown, M.A., Wallace, C.S., Angelos, M. & Truskey, G.A. Characterization of umbilical cord blood-derived late outgrowth endothelial progenitor cells exposed to laminar shear stress. *Tissue Eng Part A* **15**, 3575-3587 (2009).
24. Cao, L., Wu, A. & Truskey, G.A. Biomechanical effects of flow and coculture on human aortic and cord blood-derived endothelial cells. *J Biomech* **44**, 2150-2157 (2011).
25. Dextran Physical Properties, 2013 (Pharmacosmos; 2013).
<http://www.dextran.net/about-dextran/dextran-chemistry/physical-properties.aspx>
26. Angelos, M.G. et al. Dynamic adhesion of umbilical cord blood endothelial progenitor cells under laminar shear stress. *Biophysical journal* **99**, 3545-3554 (2010).

27. Brown, M.A. et al. The use of mild trypsinization conditions in the detachment of endothelial cells to promote subsequent endothelialization on synthetic surfaces. *Biomaterials* **28**, 3928-3935 (2007).
28. De Castro, L.M., Zennadi, R., Jonassaint, J.C., Batchvarova, M. & Telen, M.J. Effect of propranolol as antiadhesive therapy in sickle cell disease. *Clin Transl Sci* **5**, 437-444 (2012).
29. Davis, B.J., Xie, Z., Viollet, B. & Zou, M.H. Activation of the AMP-activated kinase by antidiabetes drug metformin stimulates nitric oxide synthesis in vivo by promoting the association of heat shock protein 90 and endothelial nitric oxide synthase. *Diabetes* **55**, 496-505 (2006).
30. Shaked, N.T., Satterwhite, L.L., Telen, M.J., Truskey, G.A. & Wax, A. Quantitative microscopy and nanoscopy of sickle red blood cells performed by wide-field digital interferometry. *J Biomed Optics* (**In Press**) (2011).